TRANSIENT MODELING AND TESTING OF A FLAT PLATE SOLAR COLLECTOR

by
SANDEEP JAIN

DEPARTMENT OF MECHANICAL ENGINEERING
INDIAN INSTITUTE OF TECHNOLOGY KANPUR

February, 2000

TRANSIENT MODELING AND TESTING OF A FLAT PLATE SOLAR COLLECTOR

A Thesis Submitted

in Partial Fulfillment of the Requirements

for the Degree of

Master of Technology

by

SANDEEP JAIN

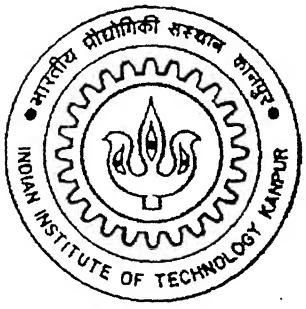

to the

DEPARTMENT OF MECHANICAL ENGINEERING

INDIAN INSTITUTE OF TECHNOLOGY KANPUR

February, 2000

CERTIFICATE

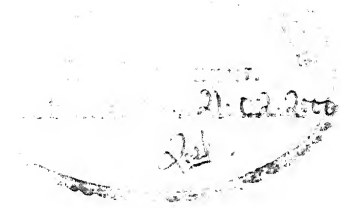

It is certified that the work contained in the thesis entitled **"Transient Modeling and Testing of a Flat Plate Solar Collector"**, by **Mr. Sandeep Jain**, has been carried out under my supervision and this work has not been submitted elsewhere for a degree.

Keshav Kant

Feb 21, 2000

(Dr. Keshav Kant)

Professor,

Department of Mechanical Engineering,

Indian Institute of Technology,

Kanpur.

February, 2000.

Acknowledgements

I express my deep sense of gratitude to my ever loving guide Dr. Keshav Kant for his excellent guidance, invaluable suggestions, constant support and encouragement during the tenure of this thesis work. It was a great pleasure to work under him as a lot of care with personal touch was available throughout.

I express my appreciation and indebtedness to my friend - Piush, Nrependra, Vivek, Vikas, Praveen, Manish, H.K. Paliwal, Sharad, Suneet, Kamlesh, Sameer, Ashish, Arvind and others, who apart from making my stay at kanpur pleasent and memorable, also helped me in my work from time to time.

Last but not the least I would like to express my greatfulness to all those who directly or indirectly helped me through sucessful completion of my work.

Sandeep Jain

Contents

List of Figures

Nomenclature

A	area, m^2
abs	absorbed
C	specific heat at constant pressure, J kg^{-1} K^{-1}
D_i	inner diameter of pipe, m
D_o	outer diameter of pipe, m
h	heat transfer coefficient, W m^{-2} K^{-1}
i,j,k	indicator of i, j and k^{th}spatial position in x,y and z directions respectively
k	thermal conductivity, W m^{-1} K^{-1}
I_t	solar radiation flux on the tilted collector per unit area, W m^{-2}
$\dot{m}$	total fluid mass flow rate, kg s^{-1}
n	number of nodal points
q	heat flux, W m^{-2}
Q	rate of heat transfer, W
P	perimeter, m

S	amount of heat flux absorbed by the absorber plate, W m^{-2}
t	time, s
V	volume, m^3
F'	collector efficiency factor
q_u	useful heat gain rate
U_l	overall loss coefficient
T_{fm}	mean of inlet and outlet temperature
$U_{T_{fi}}$,$U_{T_{fo}}$	uncertainty in measurement of inlet and outlet temperature
U_V,U_t	uncertainty in measurement of volume and time
$U_{\dot{m}}$	uncertainty in mass flow rate
U_η	uncertainty in efficiency
B_i	biot number
x,y,z	spatial coordinates

Greek Symbols

α	absorptivity of absorber plate
β	collector tilt, radian
γ	surface azimuthal angle, radian
δ	thickness, m

emissivity

latitude, radian

reflectivity; density, kg m^{-3}

angle of incidence of radiation on a tilted surface, radian

refraction angle for cover2, radian

refraction angle for cover1, radian

angle of incidence of radiation on a horizontal surface, radian

transmissivity of glass cover

Stefan-Boltzmann constant, $5.67*10^{-8}$ W m^{-2} K^{-4}

efficiency

$1*10^{-5}$

Subscripts

ambient

beam

cover2

cover1

diffuse

fluid

insulation, inlet conditions

mean

output conditions

absorber plate

wind

Abstract

The objectives of present work were to develop a multidimensional transient model of a flat plate solar collector to predict its performance and conduct experiments to validate the model.

The performance of flat plate solar collector depends upon solar insolation, latitude, time of day, angle of tilt, mass flow rate and inlet fluid temperature. The model developed here can incorporate the effect of all the above factors to predict the performance of a flat plate solar collector. The flat plate solar collector was designed, fabricated and tested on different days with different mass flow rates, angles of tilt and with varied distance between the absorber plate and the cover glass plate and also that between the two covers in a double cover design. The model was validated with the experiments conducted on the collector.

The model equations were developed considering different elements like covers, absorber plate, insulation, fluid etc. which were coupled in a global algorithm. These equations were solved using finite difference technique and computed results showed that (a) Rise in fluid temperature was maximum between 12 noon and 1P.M. (b) Plate mean temperature was maximum between 1 P.M. to 2 P.M. (c) The mean efficiency of collector decreased as the inlet fluid temperature was increased. (d) The mean efficiency was constant for flow rate greater than 40 kg/h which indicated the minimum flow rate for the collector. (e) The theoretical results were in good agreement with the experimental data from 9 A.M. to 2 P.M. which implied that transient model developed here was validated by the experimental results. This model therefore could be used to characterize a flat plate solar collector as the function of all the relevant parameters.

Chapter 1

INTRODUCTION

1.1 Need for alternative source of energy

The world population is growing fast. People around the world are demanding more and more energy as they aspire to raise their standard of living which is directly associated with the energy consumed. Nations consuming more energy on a per capita basis have better living standard than the others. Because of this natural desire to improve living standards, world energy consumption is increasing at a faster rate than world population [35].

Energy is the major infrastructure requirement for any developing or developed country. Today most of the world's energy demand is met by fossil fuels, mainly petroleum and natural gas. Enormously growing demand for energy and increasing exploitation of the available conventional energy resources is causing a rapid depletion in their reserves, which may thus not last for a long time. Conventional energy sources are polluting and leading in global pollution and global warming. There has been growing interest in the development of alternative energy sources because of global pollution, rising prices and limited reserves of fossil fuels. Solar energy, wind energy, biomass energy and tidal energy etc. are few of the available alternative energy sources.

While the potential for energy generation from these sources is immense, one of the promising option is to make more extensive use of energy derived from the sun.

1.2 Solar energy

Taking a global energy perspective, it is felt that solar energy is one of the most promising alternate sources because of its world wide availability particularly in countries lying within 35° N and 35° S latitudes. Solar energy has a great future in the tropical country like India, where many places receive a peak solar flux of the order of 1 kW/m^2 [19]. In principle, solar energy could supply all the present and future energy needs of the world on a continuing basis. Solar energy, unlike fossil fuels and nuclear power, is an environmentally clean source of energy. Another advantage is that it is free of cost and available in abundance in a large number of countries of the world.

There are also problems associated with proper utilization of solar energy. It is intermittent, low density and conversion to the electrical power is not very efficient. Solar energy can be used both directly and indirectly. It can be used directly in a variety of thermal applications like heating water or air, drying, solar distillation and cooking. The heated fluids can in turn be used for applications like power generation or refrigeration. A second way in which solar energy can be used directly is through the photovoltaic effect in which it is converted to electrical energy. Indirectly, the sun causes winds to blow, plants to grow, rain to fall and temperature differences to occur from the surface to the bottom of the oceans. Useful energy can be obtained for commercial and noncommercial purposes through all these renewable sources.

1.3 Solar collectors and their main components

In the last few decades, new solar collectors of different shapes have come up. The three most prevalent collector types are flat plate, evacuated tube, and concentrating type. The flat plate collectors have evoked considerable interest because they are the simplest among the solar energy collecting devices, least expensive and have a wide range of potential for heating and cooling applications. A schematic diagram of a flat plate solar collector is shown in Fig. 1.1. They usually consists of the following components :

1. Absorber plate

An absorber plate is generally a metal sheet of high thermal conductivity. It is coated with black paint or given a special coating so that it absorbs the incident solar radiation efficiently and loss of heat by radiation from the absorber plate is minimized. An absorber plate absorbs the incident solar radiation, converts it into heat and conducts the heat to the fluid passages.

2. Cover plate

A glass sheet of good quality which is transparent to the incoming solar radiation is fixed above the absorber plate. This prevents convective heat loss from the absorber plate and prevents infra-red radiation from the plate to escape to the atmosphere. The cover plate may be one or more in number.

3. Fluid

The heat transfer fluid is required to remove the heat from the point of collection and transferring it to the point of application. It is a means to extract the heat absorbed

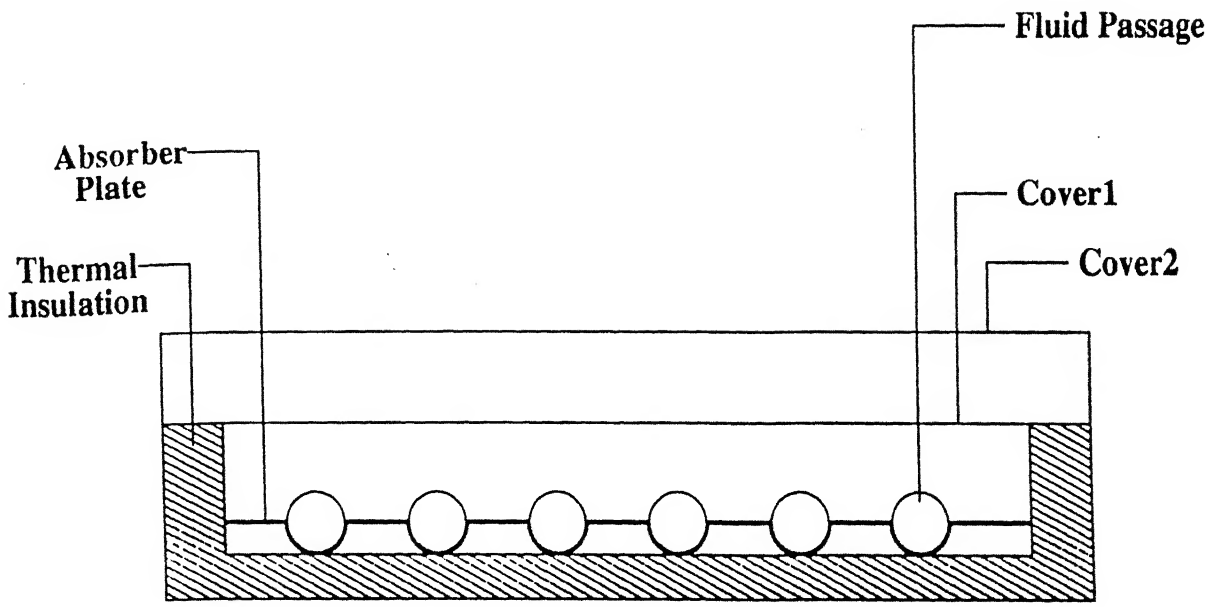

Figure 1.1: **Schematic Diagram of a Flat Plate Solar Collector**

by the absorber plate. This hot fluid may directly be used for heating purposes or may transfer its heat to another secondary fluid through a heat exchanger.

4. Insulation

The bottom and side part of the absorber plate is separated from the ambient conditions by means of a layer of insulation material. This insulation prevents the loss of heat by the plate to the surroundings. Usually the insulation used is fiberglass, glass wool, wood shavings, Styrofoam, saw dust, urethane, thermocole etc.

5. Collector box

An enclosing box whose principal functions is to hold the other components of the collector in their relative positions and to protect the collector plate and insulation material from the weather.

1.4 Scope of present work

The objectives of the present work are :

- To develop a multidimensional transient model of a flat plate solar collector to predict its performance.
- To conduct experiments to validate the model.

The performance of a flat plate solar collector depends upon the solar insolation, latitude, time of day, angle of tilt, mass flow rate and inlet fluid temperature. The model developed here attempts to incorporate the effect of all these factors and is validated by experimental data.

Chapter 2

LITERATURE SURVEY

2.1 General remarks

The solar radiation reaching the earth's surface in any location varies considerably with atmospheric conditions, hour of day and season of year, with the result that solar heat collectors always operate in an unsteady mode. The absorber plate acts as a fin to conduct heat to working fluid in collector tubes, implying the existence of thermal gradients in the plate near the tube, in direction normal to the fluid flow. Hence, at any time, the absorber plate also operates in a nonisothermal mode.

The transient modeling of a collector in a solar heating system is important since an accurate calculation of the collector's performance provides information for the assessment of the collector system for the systematic investigation of collector design and for understanding of solar energy contribution in the passive heating of buildings [36].

2.2 Review of published work

The first noticeable work available in literature in connection with flat-plate collector was by Hottel and Woertz [14]. They developed one dimensional steady state model for thermal behavior of a solar collector. The interaction between the incoming solar radiation absorbed by the covers and outgoing loss was neglected. Gutierrez et al. [11] used hybrid computer to simulate solar water heating systems using specified storage. They examined the effect of three types of auxiliary heating systems with three tanks of different size at various time distribution and loads. Klein et al. [17] investigated the effect of thermal capacitance in the modeling of the performance of a flat-plate collector. They investigated the three different models, a quasi-steady-state model with zero capacitance, second one with a single value of thermal capacitance and a third model dividing collector into many isothermal segments, or nodes. They showed that for hourly meteorological data, the zero capacitance model was adequate. Klein et al. [18] described the simulation of dynamic behavior of transient solar energy system by solving sets of differential and algebraic equations. De Ron [8] developed the model for a flat-plate solar collector considering dynamic effect. His verification and estimation procedure for the model proved to be a useful tool for comparing various collectors. Morrison and Ranatunga [21] investigated the response of thermosyphon solar water heaters to step changes of insolation. They developed a mathematical model to simulate the transient performance and measurement of the transient flow development in a thermosyphon circuit. Hobson and Norton [13] conducted detailed analysis for the heat transfer and fluid flow within direct thermosyphonic solar energy water heaters. The collector energy equations were cast in a two-dimensional form in order that heat transfer and thermal capacitance effects were simulated accurately at the small flow rates encountered commonly in these buoyancy driven systems. Saito et al. [28] presented numerical solutions for a transient one dimensional model of a solar water heater. Pier-

son and Padet [26] described a method to calculate the time constant of solar collector. They proposed an analytical expression based on experimental observations and on a thermal analysis in unsteady state. They also studied the influence of collector parameters on time constant. This helps in comparing the transient performances of different solar collectors. Chiou [5] presented a two-dimensional steady state model to study the effect of nonuniformity in the fluid flow distribution on the performance of a flat plate solar collector. Oliva and Costa [24] presented a numerical simulation of solar collectors in which they considered the effect of nonuniform and unsteady boundary conditions. They also studied the influence of shadows due to external obstacles and cover supports to the collector. Zhao et al. [36] presented a computer model derived from the basic laws governing thermal energy exchanges between surfaces for transient simulation of flat plate collectors. The approach of subdivision along the collector was used in the development of energy equations on each of the surfaces in the collector. The model was validated with experimental data. Onyegegbu and Morhenne [25] presented an unsteady two-dimensional analysis of a flat-plate solar collector subjected to time varying insolation with considerable diffuse components as a better characterization of practical solar collectors. Their analysis considered the thermal masses of absorber, tube, glazing , and the working fluid in the system and also the different optical and thermodynamic properties of beam and diffuse radiation. Srivastava and Kant [30] studied multidimensional transient analysis for single glazing .

Iqbal [15] studied the effects of free convection superimposed on forced flow in inclined tubes of a solar collector. The theoretical analysis considered fully developed Laminar flow under uniform heat flux condition and constant pressure gradient. Choudhury [6] discussed simple and efficient parameterization of insolation under partially cloudy sky and compared it with a set of exact radiative transfer results. The albedo of the earth-atmosphere system was also formulated and compared with a set

of exact radiative transfer results. Gani and Symons [10] studied the simulation of the influence of cover design on the thermal performance of flat-plate solar collectors for use at temperature of 150°C. They presented detailed results of the effect of changes in cover materials, cover surface treatments, cover system configuration and absorber plate surface treatment on both the instantaneous efficiency and the long term solar contribution of flat-plate collectors. They showed that flat plate collectors of single high transmittance cover, a convection suppressing device such as a honeycomb and selective absorber surface yielded long term solar contributions comparable to those of evacuated tubular collectors where as other simulated configurations (single or multiple cover systems) were significantly inferior. Bhide et al. [3] presented a simplified method for the comparison of thermal performance of two similarly fabricated flat plate collectors with absorber coated with coatings of known solar absorptivity and emissivity. They essentially determined the insolation values at which the two collectors gave the same thermal performance. Curves were presented which could be directly utilized by the designer for selecting the coating having better thermal performance. Thomas et al. [33] analyzed angular response measurement for four different types of collector, each type tested in three different laboratories. An analysis of the measurement procedure showed that experimentally determined angular response parameters were subjected to relatively large uncertainties. Morrison et al. [20] investigated the effect of load draw-off pattern and auxiliary boosting on the performance of vertical and horizontal tank solar water heaters. The primary factor governing the dependence of performance on load pattern in single tank systems was conduction between the auxiliary boosted zone and the solar preheat zone. A method for quantifying the effect of conduction in solar tanks was presented. Behnia and Morrison [2] investigated free convective flow and thermal structures in an open ended inclined cylindrical thermosyphon with the application to an evacuated tubular solar collector. The flow structure was visualized

using dye and rhescopic tracer particles and temperature measurements were made by a traversing thermocouple rake. Garg [12] studied the effect of dirt on the transmittance of solar radiation through various glass plates and plastic films, which are used as a transparent cover for flat-plate collectors. The dirt correction factor for glass plate inclined at an angle of 45 deg from horizontal was 0.92. The correction factor was greater for the plastic film as compared to that for the glass plate for any inclination.

Russell and Guven [27] studied all-plastic liquid flat-plate collector. Such a collector eliminates the need for coatings, metals, and all other materials except plastics. The concept appears to offer possibilities for the mass production of a low-cost, lightweight solar collectors which will be reasonably efficient. Mathematical models were developed for study of this concept. A model panel was fabricated, and computer results were compared with the experimental data for the efficiency of the panel. Nayak et al. [22] studied on solar concrete collectors used for providing domestic hot water. Although they are less efficient, yet such collectors integrated with building structures are likely to be more cost effective than conventional flat-plate collectors which use metallic absorber plates. The collectors are made up of thin concrete slabs with a network of PVC tubes embedded inside concrete. A layer of galvanized iron wiremesh on either side of the PVC tubes provides the necessary reinforcement to the concrete. The top of the slab was painted black and glazed, while the back insulation was made of autoclave cellure concrete. Nordgaard and Beckman [23] presented a new method for predicting the radiative transfer in an absorbing and isotropically scattering, non gray plane-parallel atmosphere. The technique was based upon the F ("F-hat") concept and developed to determine the radiative transfer at short wavelengths for the transparent insulation material monolithic silica aerogel. The performance of a system using aerogel collectors was compared with system using other types of high performing collectors.

Jenkins and Hill [16] compared flat plate water-heating solar collectors using the

BSE and ASHARE test procedures. Five solar collectors were tested according these procedures and the results were compared. These collectors were modular, flat-plate, water-heating, and included single and double-glazed designs with or without selectively coated absorber plates. In both procedures, collector efficiency curves were plotted. The ASHARE procedures consisted exclusively of outdoor testing whereas the BSE procedures required a combinations of outdoor and indoor testing (no irradiation) to determine the collector's optical and thermal loss characteristics, respectively. During the indoor testing in this study, the environmental test conditions were controlled and regulated by use of specially built environmental simulators and thus the effect of wind speed and "sky" temperature on the thermal loss characteristics of the collectors were investigated.

Amar et al. [1] presented the review of the literature on the test methods of flat-plate solar collectors under varying environmental conditions. The methods were examined critically from the point of view their (a) experimental procedures, (b) techniques of parameter identification and (c) output results.

2.3 Transient test methods for flat plate solar collector

Transient methods for testing flat-plate collector can be classified into the following six groups based on their similarities in approach (1) simple methods, (2) indoor methods, (3) multi-node methods, (4) multi-test methods, (5) response function methods and (6) unvalidated methods

(a) Simple methods

Arranovitch (1977) developed methods that simply added the thermal capacity term of the collector to its steady state energy balance. The performance equation, in terms of mean fluid temperature was thus given by

$$q_u = F'(\tau\alpha)_e I_T - F'U_l(T_{fm} - T_a) - (mc)\frac{dT_{fm}}{dt} \tag{2.1}$$

The thermal efficiency of the collector was calculated as

$$\eta = \frac{q_u + (mc)(dT_{fm}/dt)}{I_T} = F'(\tau\alpha)_e - F'U_l\frac{(T_{fm} - T_a)}{I_T} \tag{2.2}$$

The efficiency was plotted against the term $\frac{(T_{fm}-T_a)}{I_T}$ to give the collector parameters. The method did not require controlling the inlet fluid temperature, but an additional experiment was necessary to determine the value of (mc). The following limiting condition was usually considered :

$$\frac{dT_{fm}}{dt} \leq 12°Ch^{-1} \tag{2.3}$$

in order to keep the term $[(mc)\frac{dT_{fm}}{dt}]$ relatively small compared to q_u. The method was thus applicable to slowly varying insolation for which eqn (2.3) could be satisfied. This was clearly a limitation on the use of this method; consequently , it did not have universal applicability.

Perers (1993) described a method which considered: (a) a one-node capacitance term to include the dynamic effects and (b) separate incidence angle modifiers for direct and diffuse radiation. The technique of multiple regression analysis was suggested for estimation of collector parameters. The methods were implemented in the testing of an 11 m^2 long ground based (LGB) flat-plate collector and the results for collector

values for optical efficiencies and heat loss coefficients. This was attributed to the inaccurate expression for incidence angle modifiers and an incomplete second order model (Perers et al. ,1990; Perers and walletun, 1991). Further, scrutiny of the results presented by Perers and Walletun (1991) showed significant fluctuations in the values for effective heat capacity terms from different test runs.

Souproun (1992) proposed a transient procedure for testing a flat-plate collector. It was based mainly on the analysis of a single experimental curve consisting of a heating and subsequent cooling process. This curve was obtained from long heating period of approximately 90 min or until temperature of the heat transfer fluid exceeded 60°C, whichever was achieved first. Then the cooling process was executed by shielding off the sun. During both heating and cooling processes, solar radiation and ambient conditions remained same. Analyzing this curve, the heat losses and thermal efficiency of the collector were calculated as functions of the ratio of the heating to cooling times required to cause a temperature change between certain levels.

A sufficiently long period of steady solar insolation was required to conduct the heating process. But, such steady periods occur infrequently during variable weather. Thus, the method was not recommended for outdoor testing. It could be adopted only if a solar simulator was available.

(b) Multi-node methods

Wijeysundera and Hawlader (1984) and Hawlader and Wijeysunder (1987) proposed a two-node model for the collector in which the cover capacitance was lumped with the plate while the fluid was treated separately. The Laplace transform technique was used for obtaining expressions for plate and fluid temperatures. The experiment was carried out by shielding the collector from the sun and suddenly circulating a stream of hot fluid through it. The variation of the temperature of the plate (mid

point) and fluid (outlet) with time was monitored continuously. With an assumed set of collector parameters, theoretical results were obtained and compared with the experimental measurements. The procedure was continued until the best agreement with the experimental measurements was obtained.

With this method, no different restrictions were placed on the assumed values of the parameters; consequently, a large number of iterations were required. There was no guarantee that all guessed values were correct; different combinations of guessed values could lead to the same results and hence method was not dependable. Further, the author's results showed that a reasonable agreement was obtained for plate temperature, but fluid outlet temperature differs substantially from the experimental measurements. For such experiments high accuracy of measurement of temperature rise was needed.

Kamminga (1985a) developed a four node model (cover, plate, fluid and insulation) to describe the transient behavior of flat-plate solar collectors. An approximate solution was obtained for the fluid temperature within the collector. In a later work (Kamminga, 1985b), the model was simplified by considering three nodes (cover, plate & fluid).Finite Fourier transformation was applied to time varying differential equations leading to relations for collector characteristics. Using a series of experimental measurements at a fixed fluid inlet temperature, the collector parameters were determined by least squares methods.

According to the author, the method led to error if Fourier variables were not chosen properly. Only a limited range of time interval and Fourier variables led to appropriate equation which were amenable to inverse Fourier transformation. Moreover results from different time intervals showed a relatively large scatter.

(c) Multi-test Methods

Saunier and Chungpaibulpatana (1983) and saunier et al. (1985) proposed a method in which the solar collector was connected to an auxiliary unit and was tested under zero efficiency conditions. They assumed a quadratic expression for collector heat loss. The method required day-time test during which the collector was exposed to sun, and long night-time test run when several heating and cooling cycles were applied to collector. Both test runs were conducted outdoor under natural environmental conditions. The collector performance parameters were determined using multiple nonlinear regressive technique for experimental data.

The method required (i) an additional test to determine the auxiliary unit parameters and (ii) a long, inconvenient night-time test for estimating effective heat capacity and heat loss coefficient. Moreover, according to the authors, there was significant fluctuation in the values of collector parameters obtained from different sets of test runs due to second order heat capacitance effect neglected in the one-node model (Saunier and Chungpaibulpatana ,1983).

Chungpaibulpatana and Exell (1988, 1990) modified above method to eliminate the night-time test. While the theoretical basis remains the same, the experimental procedure was changed to determine each collector parameter individually. In addition to the day-time test of saunier, two additional shading tests were introduced and a short term heating process replaced the extended heating processes. However no experimental verification of this method has been reported in the literature. On the other hand, too many tests were proposed in this method and consequently a long chain of data reduction step needed to be followed for estimating successive approximations of various terms used in calculating the collector parameters.

(d) Response function methods

Rogers (1981) outlined a method based on collector's dynamic response to actual weather conditions. This method enabled one to obtain the steady state characteristics of a flat-plate solar collector from an analysis of the experimental data. The method was adopted by British Standard Institution as a standard for transient testing [British Standard 6757 (British Standard, 1986)]. The models assumed that the thermal output of a collector during any time interval was cumulative effect of the fractions of energy gained during that interval and a few preceding intervals. It used an impulse response function to apply a proper weighting factor to solar irradiance incident on collector . Emery and Rogers (1984) implemented this method for testing three different collectors and reported that the value obtained for collector parameters were slightly lower than those given by steady state method.

The method employed an experimental approach similar to that of the ASHARE 93-86 (ASHARE, 1986) standard and hence was much simpler compared to other methods. However, it suffered from the following disadvantages: (a) it required the handling of large data sets (b) consequently, the amount of computation was extensive (c) the response function of the collector was obtained indirectly which resulted in the best fit to the acquired experimental data, (d) the method was not used extensively so far.

Wang et al. (1987) proposed a transient procedure called the filter method for rating the thermal performance of solar collectors. The model described the dynamic characteristics of the collector. The response function of the collector was determined from a separate shielding test. Based on this function, a recursive digital filter was constructed for data processing and analyzing. Although the method incorporated a simple experimental procedure, it required familiarity with digital signal analysis and filtering.

(f) Unvalidated method

Fried (1990) proposed two-node and three-node collector models for transient test procedures. The exact solutions of the models were obtained analytically to express the collector useful heat gain in terms of its parameters and other response functions. Regression analysis was suggested to estimate collector parameters and elements of response functions. So far, these models were not implemented in any experiments.

Chapter 3

PROBLEM FORMULATION AND SOLUTION METHODOLOGY

3.1 Solar radiation

Normally measuring instruments give the values of solar radiation falling on a horizontal surface. However, most solar equipment, (e.g. flat-plate collectors) for absorbing solar radiation, are tilted at an angle to the horizontal. It therefore, becomes necessary to calculate the flux which falls on a tilted surface. Total amount of hourly global radiation reaching the tilted surface top cover is given by Sukhatme [31].

$$I_t = I_b R_b + I_d R_d + (I_b + I_d) R_r \tag{3.1}$$

where,

I_b : hourly beam radiation

I_d : hourly diffuse radiation

R_b : tilt factor for beam radiation $= \frac{cos\theta}{cos\theta_z}$

R_d : tilt factor for diffuse radiation $= \frac{(1+cos\beta)}{2}$

R_r: tilt factor for reflected radiation $= \frac{\rho(1-cos\beta)}{2}$

I_b and I_d are taken from the solar radiation data for India published by Mani [19].

Total amount of heat flux absorbed by the absorber plate is given by

$$S = I_b R_b (\tau\alpha)_b + ((I_d R_d) + (I_b + I_d) R_r)(\tau\alpha)_d \tag{3.2}$$

where,

$(\tau\alpha)_b$: transmissivity-absorptivity product for beam radiation

$(\tau\alpha)_d$: transmissivity- absorptivity product for diffuse radiation

3.2 Governing differential equations and boundary conditions

This section provides a more appropriate and accurate multidimensional transient analysis for double glazed flat plate solar collector (see Fig. 1.1). Following assumptions are made in the analysis :

1. Temperature drop through the glass covers is negligible.
2. The sky is considered as a black body.
3. Variation in all properties with respect to temperature is neglected.
4. Accumulation of dust and dirt on the collector is disregarded.
5. Shading of collector plate is not considered.
6. Temperature on periphery of the pipe is considered to be same as that of the absorber plate.

3.2.1 Cover2

The cover thickness is so small that it is reasonable to consider a uniform temperature throughout. (The lumped heat capacity approach also yields, $B_i < 0.1$). Hence, we get a two dimensional distribution of temperature , $T_{c2}(x, y)$, in cover2. The governing equation can be obtained from an energy balance in a small volume of thickness, δ_{c2}, of the cover2 as,

$$k_{c2}[\frac{\partial^2 T_{c2}}{\partial x^2} + \frac{\partial^2 T_{c2}}{\partial y^2}] + \frac{q_{a-c2}}{\delta_{c2}} + \frac{q_{c1-c2}}{\delta_{c2}} + q_{abs} = \rho_{c2} C_{c2} \frac{\partial T_{c2}}{\partial t} \tag{3.3}$$

where,

ρ_{c2} : density of cover2

C_{c2} : specific heat of cover2

k_{c2} : thermal conductivity of cover2

q_{a-c2} : heat flux from ambient to cover2

= convective heat flux (from ambient to cover2) +

radiative heat flux (from ambient to cover2)

$= h_w(T_a - T_{c2m}) + \sigma\epsilon_{c2}(T_{sky}^4 - T_{c2m}^4)$

q_{c1-c2} : heat flux from cover1 to cover2

= average convective heat flux (from cover1 to cover2) +

average radiative heat flux (from cover1 to cover2)

$= h_{c1-c2}(T_{c1m} - T_{c2m}) + \frac{\sigma(T_{c1m}^4 - T_{c2m}^4)}{(\frac{1}{\epsilon_{c1}} + \frac{1}{\epsilon_{c2}} - 1)}$

q_{abs} : heat absorbed by cover2 per unit volume $= I_t \frac{[1 - exp(-\frac{K\delta_{c2}}{cos\theta_1})]}{\delta_{c2}}$

The symbols T_a, T_{c1m}, T_{c2m}, ϵ_{c1}, ϵ_{c2} and K stand for ambient temperature, mean cover1 temperature, mean cover2 temperature, emissivity of cover1, emissivity of cover2 and extinction coefficient of cover glass 2 respectively. An empirical expression for convective heat transfer coefficient between cover2 and ambient, h_w, proposed by Sparrow and Tien has been used [29]. The symbol h_{c1-c2} stands for convective heat transfer

coefficient between cover1 and cover2 and is obtained by using the empirical expression suggested by Buchberg et al. [4]. The heat absorbed by cover, q_{abs}, is calculated using Bouger's law for a partially transparent medium [9].

It may be noted that the thermal radiation term from ambient to cover is calculated considering the ambient air as a black body which emits at sky temperature. The sky temperature is calculated from empirical relation given below [31] :

$T_{sky} = T_a - 6$

Boundary condition is taken as Adiabatic (Neumann type), i.e. :

$$\frac{\partial T_{c2}}{\partial n} = 0 \tag{3.4}$$

3.2.2 Cover1

As in the case of the cover2, here also we consider a two dimensional variation in the temperature of the cover1 i.e., $T_{c1}(x, y)$. The governing equation can be obtained from an energy balance in a small volume of thickness, δ_{c1}, of the cover1 as,

$$k_{c1}[\frac{\partial^2 T_{c1}}{\partial x^2} + \frac{\partial^2 T_{c1}}{\partial y^2}] + \frac{q_{c2-c1}}{\delta_{c1}} + \frac{q_{p-c1}}{\delta_{c1}} + q_{abs} = \rho_{c1} C_{c1} \frac{\partial T_{c1}}{\partial t} \tag{3.5}$$

where,

ρ_{c1} : density of cover1

C_{c1} : specific heat of cover1

k_{c1} : thermal conductivity of cover1

q_{c2-c1} : heat flux from cover2 to cover1

= average convective heat flux (from cover2 to cover1) +

average radiative heat flux (from cover2 to cover1)

$= h_{c1-c2}(T_{c2m} - T_{c1m}) + \frac{\sigma(T_{c2m}^4 - T_{c1m}^4)}{(\frac{1}{\epsilon_{c1}} + \frac{1}{\epsilon_{c2}} - 1)}$

q_{p-c2} : heat flux from plate to the cover1

= convective heat flux (from plate to cover1) +

radiative heat flux (from plate to cover1)

$= h_{p-c1}(T_{pm} - T_{c1m}) + \frac{\sigma(T_{pm}^4 - T_{c1m}^4)}{(\frac{1}{\epsilon_{c1}} + \frac{1}{\epsilon_p} - 1)}$

q_{abs} : heat absorbed by cover1 per unit volume $= I_t \frac{[1-exp(-\frac{K\delta_{c1}}{cos\theta_2})]}{\delta_{c1}}$

The symbols T_{c1m}, T_{c2m}, T_{pm}, ϵ_{c1}, ϵ_p and K stand for mean cover1 temperature, mean cover2 temperature, mean temperature for absorber plate ,emissivity of cover1, emissivity of plate and extinction coefficient of cover glass 1 respectively. The symbol h_{p-c1} stands for convective heat transfer coefficient between plate and cover1 and is obtained by using the empirical expression suggested by Buchberg et al. [4].

Boundary condition is taken as adiabatic (Neumann type), i.e. :

$$\frac{\partial T_{c1}}{\partial n} = 0 \tag{3.6}$$

3.2.3 Absorber plate

As in the case of the covers, here also we consider a two dimensional variation in the temperature of the absorber plate i.e., $T_p(x, y)$. The governing equation can be obtained from an energy balance in a small volume of thickness, δ_p, of the plate as,

$$k_p[\frac{\partial^2 T_p}{\partial x^2} + \frac{\partial^2 T_p}{\partial y^2}] + \frac{q_{c1-p}}{\delta_p} + \frac{q_{i-p}}{\delta_p} + \frac{q_{f-p}}{\delta_p} + \frac{S}{\delta_p} = \rho_p C_p \frac{\partial T_p}{\partial t} \tag{3.7}$$

where,

ρ_p : density of the absorber plate

C_p : specific heat of the absorber plate

k_p : thermal conductivity of the absorber plate

S : solar flux absorbed by the absorber plate

q_{p-c1} : heat flux from cover1 to the plate

= average convective heat flux (from cover1 to plate) +

average radiative heat flux (from cover1 to plate)

$= h_{p-c1}(T_{c1m} - T_{pm}) + \frac{\sigma(T_{c1m}^4 - T_{pm}^4)}{(\frac{1}{\epsilon_{c1}} + \frac{1}{\epsilon_p} - 1)}$

q_{i-p} : heat flux from insulation to absorber plate $= -k_i \frac{\partial T_i}{\partial z} \mid_{z=\delta_i}$

q_{f-p} : heat flux from fluid to absorber plate $= h_f(T_f - T_p)$

Heat transfer coefficient between plate and fluid, h_f, is calculated using the assumption of fully developed laminar flow through the pipe and constant heat flux condition [15].

Boundary condition is taken as Adiabatic (Neumann type), i.e :

$$\frac{\partial T_p}{\partial n} = 0 \tag{3.8}$$

3.2.4 Insulation

The temperature distribution $T_i(x, y, z)$ in the insulation is considered to be three dimensional (Lumped heat capacity method cannot be applied as, $B_i > 0.1$). The governing differential equation is obtained from an energy balance in a small volume of thickness δ_i, of the insulation as,

$$k_i[\frac{\partial^2 T_i}{\partial x^2} + \frac{\partial^2 T_i}{\partial y^2} + \frac{\partial^2 T_i}{\partial z^2}] = \rho_i C_i \frac{\partial T_i}{\partial t} \tag{3.9}$$

where,

ρ_i : density of the insulation

C_i : specific heat of the insulation

k_i : thermal conductivity of the insulation

There is no heat generation or absorption inside the insulation. The boundary conditions are:

Faces exposed to the atmosphere (Robin's type B.C.) :

$$-k_i(\frac{\partial T_i}{\partial n}) = h_w(T_i - T_a) \tag{3.10}$$

Face in contact with the absorber plate (Dirichlet type B.C.) :

$$T_i = T_p \tag{3.11}$$

3.2.5 Fluid

The fluid flow in the duct is considered to be one dimensional i.e. average values of temperature, T_f, are used in each cross sectional area of the fluid stream. The governing differential equation of the fluid flow is :

$$\rho_f A_f C_f \frac{\partial T_f}{\partial t} = q_{p-f} P - \dot{m} C_f \frac{\partial T_f}{\partial x} \tag{3.12}$$

where,

ρ_f : density of the fluid

C_f : specific heat of the fluid

$\dot{m}$: mass flow rate of the fluid

q_{p-f} : convective heat flux from the absorber plate to the fluid

$= h_f(T_p - T_f)$

$P = perimeter = \pi D_i$

A_f = area of cross-section $= (\frac{\pi D_i^2}{4})$

The inlet boundary condition for the fluid at x=0 , $y = 0$ is :

$$T_f = T_{fi} \tag{3.13}$$

3.3 Method of solution

The finite difference method is used to discretize the governing differential equations. The technique used for discretization is Alternative Direction Implicit (ADI) for cover2, cover1, absorber plate, insulation & Implicit scheme for fluid. In the method, the entire region is divided into small grids of finite size. Temperatures are calculated on all the nodal points at each time step as we move forward in time domain. In the nomenclature used, i, j and k represent parameters in x,y and z directions respectively and n is the parameter in time domain. The discretized elements of covers, plate, insulation and fluid of a solar collector are shown in Fig. 3.1. The computational algorithm for the coupling solution is indicated by a flowchart (Fig. 3.2). Partial derivatives are expressed in the following forms :

$$\frac{\partial T}{\partial x} = \frac{T_{i+1} - T_{i-1}}{2\Delta x} + O(\Delta x^2)$$

$$\frac{\partial^2 T}{\partial x^2} = \frac{T_{i+1} - 2T_i + T_{i-1}}{2\Delta x^2} + O(\Delta x^2)$$

$$\frac{\partial T}{\partial t} = \frac{T^{n+1} - T^n}{\Delta t} + O(\Delta t)$$

The notation $O(\Delta x^2)$ means that arriving at the above, order of (Δx^2) and higher have been neglected. $O(\Delta x^2)$ is called truncation error. Truncation error for 2-D ADI is $O(\Delta t^2, \Delta x^2, \Delta y^2)$ and for 3-D ADI it is $(\Delta t, \Delta x^2, \Delta y^2, \Delta z^2)$ [32]. Truncation error is the difference between the exact mathematical expression and the numerical expression.

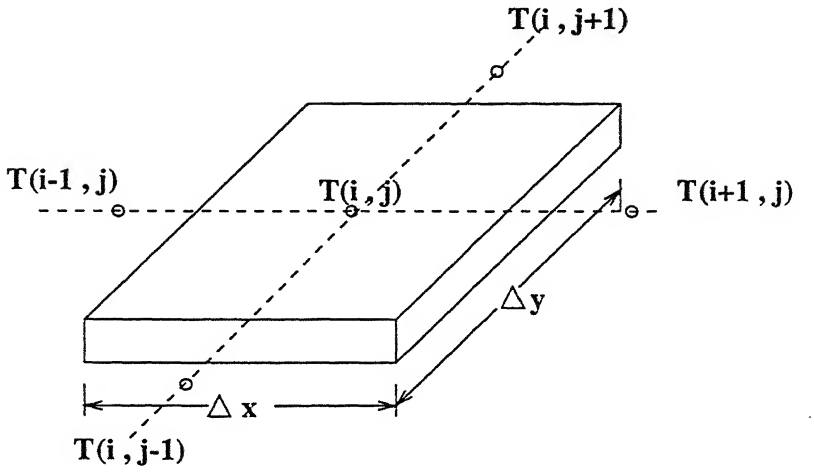

(a) Discrete grid points in covers and plate

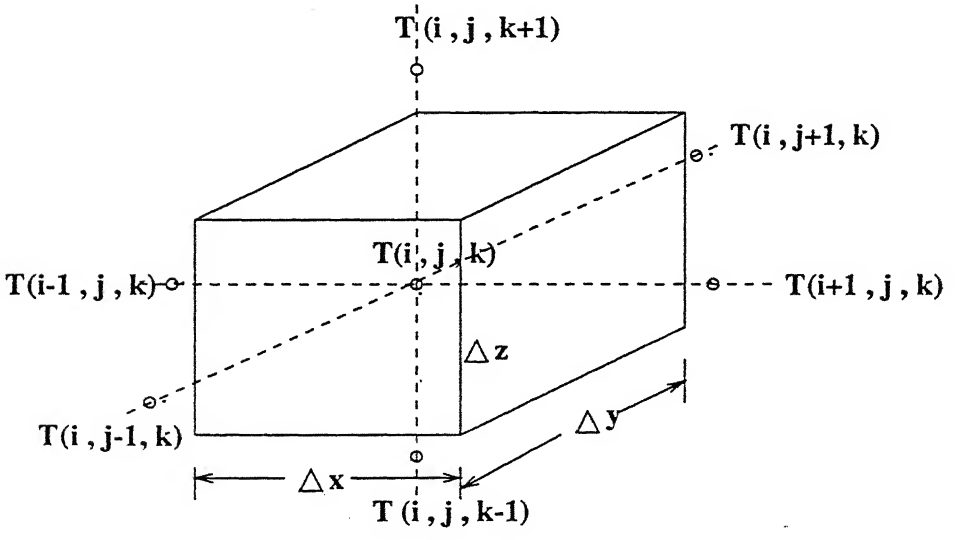

(b) Discrete grid points in the insulation

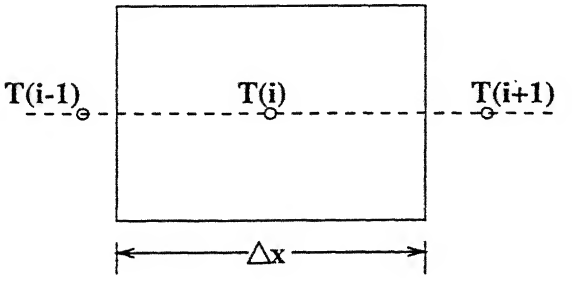

(c) Discrete grid points in fluid

Figure 3.1: Discrete Grid Points of Different Components of a Solar Collector

3.3.1 Cover2 :

A set of discretized equations is obtained by numerical approximation of the governing equation (3.3) and its boundary condition (3.4) into each one of the control volumes of the grid. The evaluation of the heat conducted is made using Alternative Direction Implicit (ADI) technique. The convection heat exchanged with outside is taken implicitly and remaining heat exchanges are taken explicitly.

Two equations are established for each point of the grid, each one implicit in one direction.

1. First implicit equation in x direction (move $\frac{\Delta t}{2}$ forward in time domain) yields

$$bT_{c2}(i-1,j,n+1/2)+dT_{c2}(i,j,n+1/2)+aT_{c2}(i+1,j,n+1/2)=r \qquad (3.14)$$

where,

$b = k_{c2}\Delta y\frac{\delta_{c2}}{\Delta x}$

$d = -[2k_{c2}\Delta y\frac{\delta_{c2}}{\Delta x}+2\rho_{c2}C_{c2}\Delta x\Delta y\frac{\delta_{c2}}{\Delta t}+h_w\Delta x\Delta y]$

$a = k_{c2}\Delta y\frac{\delta_{c2}}{\Delta x}$

$r = -k_{c2}\Delta x\frac{\delta_{c2}}{\Delta y}[T_{c2}(i,j-1,n)-2T_{c2}(i,j,n)+T_{c2}(i,j+1,n)-\Delta x\Delta y[h_wTa$

$+\sigma\epsilon_{c2}(T^4_{sky}-T^4_{c2}(i,j,n))]-\Delta x\Delta y[h_{c1-c2}(T_{c1m}-T_{c2m})+\frac{\sigma(T^4_{c1m}-T^4_{c2m})}{(\frac{1}{\epsilon_{c1}}+\frac{1}{\epsilon_{c2}}-1)}]$

$-q_{abs}\Delta x\Delta y\delta_{c2}-\rho_{c2}C_{c2}\Delta x\Delta y\delta_{c2}\frac{T_{c2}(i,j,n)}{\Delta t}$

2. Second implicit equation in y direction (move by another$\frac{\Delta t}{2}$ in time domain) yields

$$bT_{c2}(i,j-1,n+1)+dT_{c2}(i,j,n+1)+aT_{c2}(i,j+1,n+1)=r \qquad (3.15)$$

where,

$b = k_{c2}\Delta x\frac{\delta_{c2}}{\Delta y}$

$$d = -[2k_{c2}\Delta x\frac{\delta_{c2}}{\Delta y} + 2\rho_{c2}C_{c2}\Delta x\Delta y\frac{\delta_{c2}}{\Delta t} + h_w\Delta x\Delta y]$$

$$a = k_{c2}\Delta x\frac{\delta_{c2}}{\Delta y}$$

$$r = -k_{c2}\Delta y\frac{\delta_{c2}}{\Delta x}[T_{c2}(i-1,j,n+1/2) - 2T_{c2}(i,j,n+1/2) + T_{c2}(i,j+1,n+1/2)$$

$$-\Delta x\Delta y[h_wTa + \sigma\epsilon_{c2}(T^4_{sky} - T^4_{c2}(i,j,n+1/2))] - \Delta x\Delta y[h_{c1-c2}(T_{c1m} - T_{c2m}) +$$

$$\frac{\sigma(T^4_{c1m} - T^4_{c2m})}{(\frac{1}{\epsilon_{c1}} + \frac{1}{\epsilon_{c2}} - 1)}] - q_{abs}\Delta x\Delta y\delta_{c2} - \rho_{c2}C_{c2}\Delta x\Delta y\delta_{c2}\frac{T_{c2}(i,j,n+1/2)}{\Delta t}$$

The coefficient matrices of the resultant equations are tridiagonal. The coefficients a, d, b are respectively for upper diagonal, diagonal, lower diagonal elements and r is a constant vector. Therefore, it can be solved by a Tridiagonal Matrix Algorithm (TDMA). The boundary conditions in discretized form can be expressed as (by image point boundary): at

$i = 1 \qquad T_{c2}(i-1,j) = T_{c2}(i+1,j)$

$i = n_x \qquad T_{c2}(i+1,j) = T_{c2}(i-1,j)$

$j = 1 \qquad T_{c2}(i,j-1) = T_{c2}(i,j+1)$

$j = n_y \qquad T_{c2}(i,j+1) = T_{c2}(i,j-1)$

3.3.2 Cover1

A set of discretized equations is obtained by numerical approximation of the governing equation (3.5) and its boundary condition (3.6) into each one of the control volumes of the grid. The evaluation of the heat conducted is made using ADI technique. Heat exchanges on cover2 side and the plate side are calculated explicitly.

Two equations are established for each point of the grid, each one implicit in one direction.

1. First implicit equation in x direction (move $\frac{\Delta t}{2}$ forward in time domain) yields

$$bT_{c1}(i-1,j,n+1/2)+dT_{c1}(i,j,n+1/2)+aT_{c1}(i+1,j,n+1/2)=r \qquad (3.16)$$

where,

$b = k_{c1}\Delta y\frac{\delta_{c1}}{\Delta x}$

$d = -[2k_{c1}\Delta y\frac{\delta_{c1}}{\Delta x}+2\rho_{c1}C_{c1}\Delta x\Delta y\frac{\delta_{c1}}{\Delta t}]$

$a = k_{c1}\Delta y\frac{\delta_{c1}}{\Delta x}$

$r = -k_{c1}\Delta x\frac{\delta_{c1}}{\Delta y}[T_{c1}(i,j-1,n)-2T_{c1}(i,j,n)+T_{c1}(i,j+1,n)-\Delta x\Delta y[h_{c1-c2}$
$(T_{c2m}-T_{c1m})+\frac{\sigma(T^4_{c2m}-T^4_{c1m})}{(\frac{1}{\epsilon_{c1}}+\frac{1}{\epsilon_{c2}}-1)}]-\Delta x\Delta y[h_{p-c1}(T_{pm}-T_{c1m})+$
$\frac{\sigma(T^4_{pm}-T^4_{c1m})}{(\frac{1}{\epsilon_{c1}}+\frac{1}{\epsilon_{p}}-1)}-q_{abs}\Delta x\Delta y\delta_{c1}-2\rho_{c1}C_{c1}\Delta x\Delta y\delta_{c1}\frac{T_{c1}(i,j,n)}{\Delta t}$

2. Second implicit equation in y direction (move by another $\frac{\Delta t}{2}$ in time domain) yields

$$bT_{c1}(i,j-1,n+1)+dT_{c1}(i,j,n+1)+aT_{c1}(i,j+1,n+1)=r \qquad (3.17)$$

where,

$b = k_{c1}\Delta x\frac{\delta_{c1}}{\Delta y}$

$d = -[2k_{c1}\Delta x\frac{\delta_{c1}}{\Delta y}+2\rho_{c1}C_{c1}\Delta x\Delta y\frac{\delta_{c1}}{\Delta t}]$

$a = k_{c1}\Delta x\frac{\delta_{c1}}{\Delta y}$

$r = -k_{c1}\Delta y\frac{\delta_{c1}}{\Delta x}[T_{c1}(i-1,j,n+1/2)-2T_{c1}(i,j,n+1/2)+T_{c1}(i,j+1,n+1/2)]$
$-\Delta x\Delta y[h_{c1-c2}(T_{c2m}-T_{c1m})+\frac{\sigma(T^4_{c2m}-T^4_{c1m})}{(\frac{1}{\epsilon_{c1}}+\frac{1}{\epsilon_{c2}}-1)}]-\Delta x\Delta y[h_{p-c1}(T_{pm}-T_{c1m})$
$+\frac{\sigma(T^4_{pm}-T^4_{c1m})}{(\frac{1}{\epsilon_{c1}}+\frac{1}{\epsilon_{p}}-1)}]-q_{abs}\Delta x\Delta y\delta_{c1}-2\rho_{c1}C_{c1}\Delta x\Delta y\delta_{c1}\frac{T_{c1}(i,j,n+1/2)}{\Delta t}$

The coefficient matrices of the resultant equations are tridiagonal. The coefficients a, d, b are respectively for upper diagonal, diagonal, lower diagonal elements and r is a constant vector. Therefore, it can be solved by a Tridiagonal Matrix Algorithm (TDMA). The boundary conditions in discretized form can be expressed as (by image

point boundary): at

$i = 1 \qquad T_{c1}(i-1,j) = T_{c1}(i+1,j)$

$i = n_x \qquad T_{c1}(i+1,j) = T_{c1}(i-1,j)$

$j = 1 \qquad T_{c1}(i,j-1) = T_{c1}(i,j+1)$

$j = n_y \qquad T_{c1}(i,j+1) = T_{c1}(i,j-1)$

3.3.3 Absorber plate

The governing energy equation for absorber plate is (3.7). A discretized equation is obtained by numerical approximation of the governing equation, using ADI criteria. Heat exchanges on cover side and with fluid and insulation are calculated explicitly.

Two equations are established for each point of the grid, each one implicit in one direction.

1. First implicit equation in x direction (move $\frac{\Delta t}{2}$ forward in time domain) yields

$$bT_p(i-1,j,n+1/2) + dT_p(i,j,n+1/2) + aT_p(i+1,j,n+1/2) = r \qquad (3.18)$$

where,

$b = k_p \Delta y \frac{\delta_p}{\Delta x}$

$d = -[2k_p \Delta y \frac{\delta_p}{\Delta x} + 2\rho_p C_p \Delta x \Delta y \frac{\delta_p}{\Delta t}]$

$a = k_p \Delta y \frac{\delta_p}{\Delta x}$

$r = -k_p \Delta x \frac{\delta_p}{\Delta y}[T_p(i,j-1,n) - 2T_p(i,j,n) + T_p(i,j+1,n) - \Delta x \Delta y[h_{p-c1}(T_{c1m}$

$-T_{pm}) + \frac{\sigma(T_{c1m}^4 - T_{pm}^4)}{(\frac{1}{\epsilon_{c1}} + \frac{1}{\epsilon_p} - 1)}] - k_i \frac{\Delta x \Delta y}{\Delta z}[T_i(i,j,n_z - 1,n) - T_i(i,j,n_z,n)]$

$-h_f P \Delta y[T_f(i,j,n) - T_p(i,j,n)] - S\Delta x \Delta y - 2\rho_p C_p \Delta x \Delta y \delta_p \frac{T_p(i,j,n)}{\Delta t}$

2. Second implicit equation in y direction (move by another $\frac{\Delta t}{2}$ in time domain) yields

$$bT_p(i,j-1,n+1) + dT_p(i,j,n+1) + aT_p(i,j+1,n+1) = r \tag{3.19}$$

where,

$b = k_p \Delta x \frac{\delta_p}{\Delta y}$

$d = -[2k_p \Delta x \frac{\delta_p}{\Delta y} + 2\rho_p C_p \Delta x \Delta y \frac{\delta_p}{\Delta t}]$

$a = k_{c1} \Delta x \frac{\delta_{c1}}{\Delta y}$

$r = -k_p \Delta y \frac{\delta_p}{\Delta x}[T_p(i-1,j,n+1/2) - 2T_p(i,j,n+1/2) + T_p(i,j+1,n+1/2)]$

$-\Delta x \Delta y[h_{p-c1}(T_{c1m} - T_{pm}) + \frac{\sigma(T_{c1m}^4 - T_{pm}^4)}{(\frac{1}{\epsilon_{c1}} + \frac{1}{\epsilon_p} - 1)}] - k_i \frac{\Delta x \Delta y}{\Delta z}[T_i(i,j,n_z - 1,n)$

$-T_i(i,j,n_z,n)] - h_f P \Delta y[T_f(i,j,n) - T_p(i,j,n)] - S\Delta x \Delta y - 2\rho_p C_p \Delta x \Delta y \delta_p \frac{T_p(i,j,n+1/2)}{\Delta t}$

The coefficient matrices of the resultant equations are tridiagonal. The coefficients a, d, b are respectively for upper diagonal, diagonal, lower diagonal elements and r is a constant vector. It can be solved by a Tridiagonal Matrix Algorithm (TDMA). The boundary conditions in discretized form can be expressed as (by image point boundary): at

$i = 1 \qquad T_p(i-1,j) = T_p(i+1,j)$

$i = n_x \qquad T_p(i+1,j) = T_p(i-1,j)$

$j = 1 \qquad T_p(i,j-1) = T_p(i,j+1)$

$j = n_y \qquad T_p(i,j+1) = T_p(i,j-1)$

3.3.4 Insulation

The discretization is carried out by means of a regular three dimensional grid. For each one of the control volume elements, a discretized equation is obtained as a result of

numerical approximation of the governing equation (3.9) and its boundary conditions (3.10 & 3.11). ADI method is used for evaluation of the heat conduction. Three equations are obtained for each point of the grid, each one implicit in one direction.

1. First implicit equation in x direction (move $\frac{\Delta t}{3}$forward in time domain) yields

$$bT_i(i-1,j,k,n+1/3) + dT_i(i,j,k,n+1/3) + aT_i(i+1,j,k,n+1/3) = r \qquad (3.20)$$

where,

$b = k_i \frac{\Delta y \Delta z}{\Delta x}$

$d = -[2k_i \frac{\Delta y \Delta z}{\Delta x} + 3\rho_i C_i \frac{\Delta x \Delta y \Delta z}{\Delta t}]$

$a = k_i \frac{\Delta y \Delta z}{\Delta x}$

$r = -k_i \frac{\Delta x \Delta z}{\Delta y}[T_i(i,j-1,k,n) - 2T_i(i,j,k,n) + T_i(i,j+1,k,n)] - k_i \frac{\Delta x \Delta y}{\Delta z}$

$[T_i(i,j,k-1,n) - 2T_i(i,j,k,n) - T_i(i,j,k+1,n)] - 3\rho_i Ci \Delta x \Delta y \Delta z \frac{T_i(i,j,k,n)}{\Delta t}$

2. Second implicit equation in y direction (move by another$\frac{\Delta t}{3}$ in time domain) yields

$$bT_i(i,j-1,k,n+2/3) + dT_i(i,j,k,n+2/3) + aT_i(i,j+1,k,n+2/3) = r \qquad (3.21)$$

where,

$b = k_i \frac{\Delta x \Delta z}{\Delta y}$

$d = -[2k_i \frac{\Delta x \Delta z}{\Delta y} + 3\rho_i C_i \frac{\Delta x \Delta y \Delta z}{\Delta t}]$

$a = k_i \frac{\Delta x \Delta z}{\Delta y}$

$r = -k_i \frac{\Delta y \Delta z}{\Delta x}[T_i(i-1,j,k,n+1/3) - 2T_i(i,j,k,n+1/3) + T_i(i+1,j,k,n+1/3)]$

$-k_i \frac{\Delta x \Delta y}{\Delta z}[T_i(i,j,k-1,n+1/3) - 2T_i(i,j,k,n+1/3) - T_i(i,j,k+1,n+1/3)]$

$-3\rho_i Ci \Delta x \Delta y \Delta z \frac{T_i(i,j,k,n+1/3)}{\Delta t}$

3.Third implicit equation in z direction (move by another $\frac{\Delta t}{3}$ in time domain) yields

$$bT_i(i,j,k-1,n+1) + dT_i(i,j,k,n+1) + aT_i(i,j,k+1,n+1) = r \tag{3.22}$$

where,

$b = k_i \frac{\Delta x \Delta y}{\Delta z}$

$d = -[2k_i \frac{\Delta x \Delta y}{\Delta z} + 3\rho_i C_i \frac{\Delta x \Delta y \Delta z}{\Delta t}]$

$a = k_i \frac{\Delta x \Delta y}{\Delta z}$

$r = -k_i \frac{\Delta y \Delta z}{\Delta x}[T_i(i-1,j,k,n+2/3) - 2T_i(i,j,k,n+2/3) + T_i(i+1,j,k,n+2/3)]$

$-k_i \frac{\Delta x \Delta z}{\Delta y}[T_i(i,j-1,k,n+2/3) - 2T_i(i,j,k,n+2/3) - T_i(i,j+1,k,n+2/3)]$

$-3\rho_i Ci \Delta x \Delta y \Delta z \frac{T_i(i,j,k,n+2/3)}{\Delta t}$

The coefficient matrices of the resultant equations are tridiagonal. The coefficient a, d, b are respectively for upper diagonal, diagonal, lower diagonal elements and r is a constant vector. It can be solved one by one using Tridiagonal Matrix Algorithm (TDMA). The boundary conditions are : at

$i = 1 \qquad T_i(i-1,j,k) = T_i(i+1,j,k) + \frac{h_w 2\Delta x}{k_i}[T_i(i,j,k) - T_a]$

$i = n_x \qquad T_i(i+1,j,k) = T_i(i-1,j,k) - \frac{h_w 2\Delta x}{k_i}[T_i(i,j,k) - T_a]$

$j = 1 \qquad T_i(i,j-1,k) = T_i(i,j+1,k) + \frac{h_w 2\Delta y}{k_i}[T_i(i,j,k) - T_a]$

$j = n_y \qquad T_i(i,j+1,k) = T_i(i,j-1,k) - \frac{h_w 2\Delta y}{k_i}[T_i(i,j,k) - T_a]$

$k = 1 \qquad T_i(i,j,k-1) = T_i(i,j,k+1) + \frac{h_w 2\Delta z}{k_i}[T_i(i,j,k) - T_a]$

$k = n_z \qquad T_i(i,j,k) = T_p(i,j)$

3.3.5 Fluid

For each one of the finite control volumes that results by subdividing the pipe, the discretization equations are obtained by numerical approximation of energy equation (3.12). The internal energy transportation is calculated implicitly.

$$T_f(i,j,n+1) = \frac{[\dot{m}C_f\, T_f(i-1,j,n+1) + h_f\, P\Delta x T_p(i,j) + \rho_f\, A_f\, C_f\, \Delta x \frac{T_f(i,j,n)}{\Delta t}]}{[\dot{m}C_f + \rho_f\, A_f\, C_f\, \frac{\Delta x}{\Delta t} + h_f\, P\Delta x]} \tag{3.23}$$

The boundary condition is : at i=0, j=0

$$T_f(i,j) = T_{fi}$$

Equations described above yield temperature distributions in cover2, cover1, absorber plate, insulation and fluid as a function of time and spatial co-ordinate. The temperature distribution can be found out at time t+Δt if we know the temperature distribution at time t. The initial temperature of different elements of the collector is taken as the ambient temperature when the calculation is initialized. The accuracy improves when the spatial and temporal discretization densities are increased. The numerical solution tends towards an asymptotic value when finer grids are used. For the discretization used, further increment in the density of discretization does not cause appreciable improvement in the numerical solution. Two important parameters namely the stagnation temperature and efficiency of the collector are defined below.

3.4 Stagnation temperature

It refers to the condition of a flat plate solar collector when the liquid flow through the collector is stopped. There is no useful heat gain and its efficiency is zero. In this case,

absorber plate attains a temperature such that the energy absorbed by it is equal to the heat loss. This temperature is the highest that the absorber plate can attain and is called the stagnation temperature.

3.5 Efficiency

It is an important parameter to estimate the performance of a collector. The instantaneous efficiency of a flat plate solar collector is defined as the ratio of useful heat gain to the flux incident on the collector. The mean efficiency of collector is defined as the ratio of the total useful heat gain to the total incident radiation on the collector over the period of its operation. The collector efficiency based on the absorber plate area is

$$\eta = \frac{\dot{m}\, C_p\, (T_{fo} - T_{fi})}{A_p\, I_t}$$

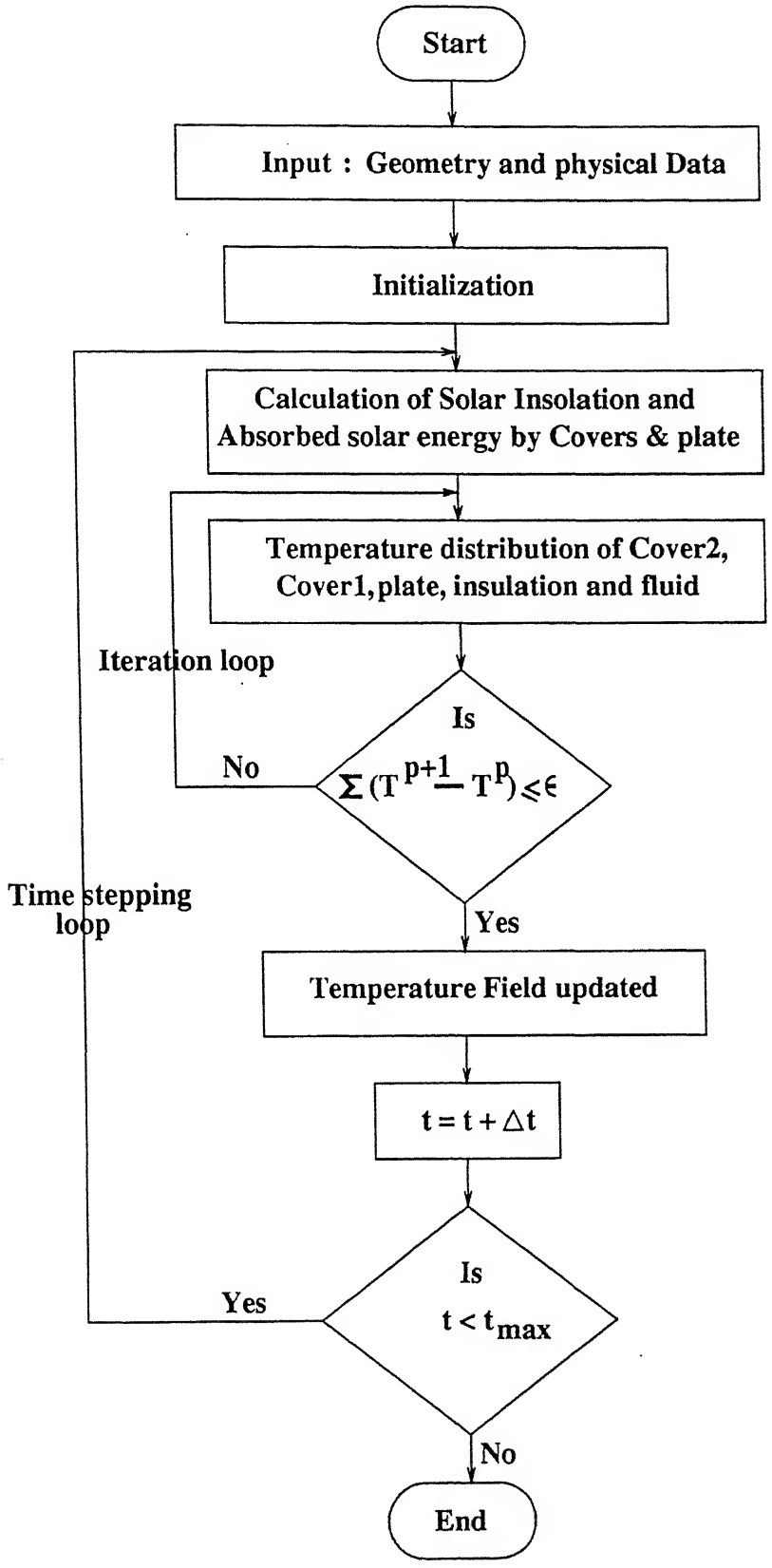

Figure 3.2: **Computational Algorithm of Numerical Solution**

Chapter 4

EXPERIMENTAL SET-UP AND TEST PROCEDURE

4.1 Purpose of experiment

The experiments were conducted with the purpose of getting real time data for validation of the theoretical model developed here for the flat-plate solar collector.

4.2 Description of experimental set-up

The experimental set-up was completed with the following major components.

1. Absorber plate
2. Cover plate
3. Insulation
4. Casing
5. Instrumentation

1. Absorber plate

The choice of material depends on the thermal properties (conductivity & capacitance), mechanical properties (density, ductility & ease of soldering/welding), corrosion resistance, cost and availability . Galvanized iron, steel, aluminum, copper, stainless steel and plastic etc. may be used as material for plate. In the present study, copper was used. Although it is expensive, but it has good thermal and mechanical properties and also corrosion resistance.

Three different types of absorber plate configurations normally used are (1) Pipe and fin (2) Full water sandwich (3) Semi water sandwich type as shown in Fig. 4.1. Pipe and fin type (all copper) configuration was taken due to its long life, low maintenance and capital cost, good corrosion resistance and its ability to withstand high pressure . The absorber used in present test rig is shown in Fig. 4.2.

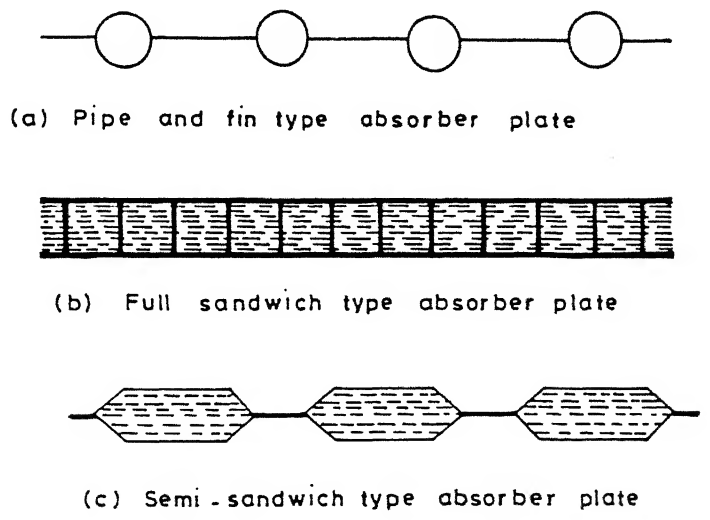

Figure 4.1: **Absorber Plate Configuration**

2. Cover plate

Glass is the most commonly used cover material. It has high transmittance (of the order of 0.85 or more) in short wavelength range and is practically opaque to long wave infrared radiation emitted by the absorber plate. Glass deterioration is negligible even over very long periods of exposure to intense ultraviolet radiation. The cover plate used for collector was made of simple window glass of 4 mm thickness.

3. Insulation

Several types of insulation materials are used in collectors to minimize the heat loss from the back and sides. The commonly used materials are fiberglass, ceramic fiber blanket, mineral fiber blanket, calcium silicate foam, urea formaldehyde foam, polyurethane foam and glass wool. Glass wool was chosen in the present case since it was inexpensive and easily available.

4. Casing

The material chosen for casing was a GI sheet of 30 gauge thickness because of good strength, good corrosion resistance, low cost and easy availability.

A complete assembly of the collector is shown in Fig. 4.3 and a line diagram of the complete test rig is shown in Fig. 4.4.

5. Instrumentation

(a) Temperature measurement

The temperature measurement was done using 24 gauge copper constantan thermocouples (supplied by Love Controls Corpn. USA). The location of thermocouples is shown in Fig. 4.2. The temperatures were recorded using direct temperature measur-

ing instrument. The thermocouples were calibrated using constant temperature water bath between 0°C and 100°C. Thermometer was used to measure the ambient, the inlet and the outlet water temperatures. The accuracy of temperature measurement was ±0.2°C.

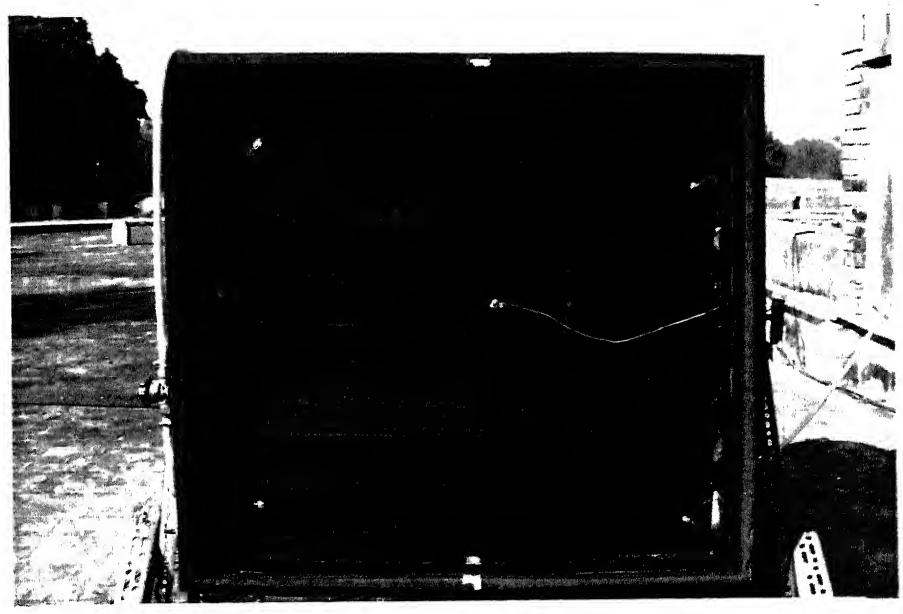

Figure 4.2: **Absorber Plate**

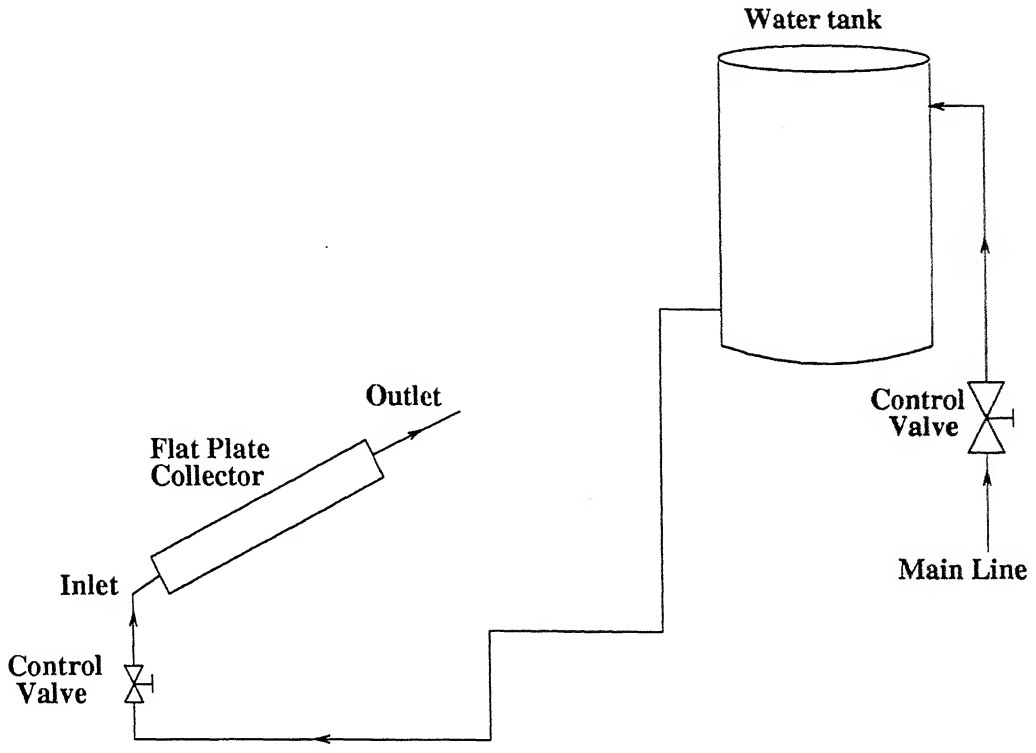

Figure 4.4: **Line Diagram of the Test Rig**

(b) Mass flow rate measurement

Mass flow rate was measured by direct measurement of volume discharged, with the help of a calibrated measuring flask. The time was taken by a stop watch (made by Hanhart, Germany). The accuracy of volume measurement was ± 5 ml and that of time was ± 0.1 s.

4.3 Fabrication and installation

Generally the shape of a solar flat-plate collector is rectangular. The fabrication of the collector was done in several stages. The main structure was started by making a rectangular box of wood of overall dimension 1.05 m$\times$1.05 m. Further the absorber plate was fixed in the structure by giving space for insulation. The insulation used in flat-plate collector was glass wool. The thickness of insulation used was 80 mm for the

back and 40 mm for the sides.

The absorber plate was made of copper material of size 1.05 m×1.0 m. To get better surface contact between plate and pipe, nine depressions made in the plate at a pitch of 85 mm, Nine copper pipes were placed in the depression and were brazed with the plate filling the depression with copper eutectic. The copper pipes were taken of 12.5 mm (1/2 inch) in diameter and these were brazed in series using elbows. They were then tested for leakage using the tap water. The upper surface of the absorber plate was painted with black board black paint. Five Thermocouples were provided at four corners and one in the middle. The final size of collector plate so obtained was 1.0 m×.95 m. Provision was made for the movement of absorber plate by screw and pinion arrangement for varying the distance between the absorber plate and the cover.

The cover plate was provided above the absorber plate which helped to prevent convective and re-radiative heat losses to the atmosphere. The option was available for using either single or double glazing. There was also provision for varying the distance between the cover plates in a double cover design. Finally the sides of the collector were covered with GI sheet of 30 gauge.

The stand for collector was fabricated, the frame of which was made of slotted angle iron. The bearing type arrangement shown in fig. 4.3 was made for the movement of the flat plate collector.

Once the solar flat-plate collector was ready. A PVC tank of 500 liter capacity was connected to the flat plate collector through proper fittings. A float valve was used to maintain a constant water level. After careful and thorough investigation, a suitable site of the set-up was decided. There was availability of electricity and water tap on the roof of heat transfer lab which was chosen for the installation. Finally, Initial testing was done to get the correct orientation and full sun shine.

4.4 Test procedure

The experiments were conducted during the winter, months namely Dec, Jan and Feb on the set-up. The opening of control valve used in the pipe line for the control of mass flow rate through the flat-plate solar collector was regulated and the temperatures readings were taken at regular intervals of one hour each from 9 A.M. to 4 P.M., on daily basis.

(a) Collector inlet

(b) Collector outlet

(c) Plate temperature at 5 different location

(d) Ambient temperature

The direct measurement of volume of water was taken at outlet of collector. The time was taken by a stopwatch for collection of water. The data were repeated for three different flow rates namely 15.5 kg/h, 31.5 kg/h and 56.5 kg/h.

The experiment was conducted only on clear days to overcome the influence of cloudiness on the incidence of solar radiation.

4.5 Experimental uncertainties

Errors in the experiment may arise due to various reasons. These can be classified as:

(a) Systematic or determinate errors, arising as a result of poor calibration of instruments and

(b) Random or unavoidable errors, arising as a result of uncertainty associated with the accuracy of measuring instrument and the ability of the operator to read such instruments both accurately and consistently.

While no attempt was done in the present study to quantify these errors, all feasible efforts within the practical limits were implemented to ensure that the possible errors

are minimized.

Uncertainty Analysis

The data reduction equation of efficiency is given by

$\eta = \frac{\dot{m}C_p(T_{fo}-T_{fi})}{A_p I_t}$

The value of $\dot{m}$, T_{fo} and T_{fi} were measured while the values of A_p and I_t were taken directly. Therefore, the efficiency depended only on $\dot{m}$, T_{fo} and T_{fi}.

i.e. $\eta = \eta(T_{fi}, T_{fo}, \dot{m})$

The uncertainty in T_{fi} and T_{fo} are 0.2°C. The uncertainty in $\dot{m}$ can be determined as follows :

$\dot{m} = \dot{m}$(V,t)

Where both V and t were measured. The uncertainty in V and t were 5 ml and 0.1 s. The uncertainty analysis expression in the measurement of $\dot{m}$ can be written as [7] :

$$\begin{aligned}(\tfrac{U_{\dot{m}}}{\dot{m}})^2 &= (\tfrac{U_V}{V})^2 + (\tfrac{U_t}{t})^2 \\ &= (\tfrac{.005}{.25})^2 + (\tfrac{.1}{58})^2 \\ &= .000403\end{aligned}$$

$(\frac{U_{\dot{m}}}{\dot{m}}) = .020007$

Uncertainty in the measurement of mass flow rate was 2.0%. The uncertainty analysis expression in the efficiency can be written as [7] :

$$\begin{aligned}(\tfrac{U_\eta}{\eta})^2 &= (\tfrac{U_{T_{fi}}}{T_{fo}-T_{fi}})^2 + (\tfrac{U_{T_{fo}}}{T_{fo}-T_{fi}})^2 + (\tfrac{U_{\dot{m}}}{\dot{m}})^2 \\ &= (\tfrac{0.2}{21})^2 + (\tfrac{0.2}{21})^2 + (.020)^2 \\ &= .0005814\end{aligned}$$

$(\frac{U_\eta}{\eta}) = .02411$

The uncertainty in efficiency was 2.41% at 12 noon for mass flow rate 15.5 kg/h.

On a particular day for a given mass flow rate, the uncertainty will vary from morning to evening because of changing solar insolation and therefore the temperature

rise. Hence one can talk about some minimum or maximum value in this situation. This uncertainty falls in the range of 2.41% to 7.35%.

At a given time of day for different mass flow rate, the uncertainty will be different on temperature rise. This value falls in the range of 2.41% to 4.51% at noon for mass flow rate in the range of 15.5 kg/h to 56.5 kg/h respectively.

Chapter 5

RESULTS AND DISCUSSION

5.1 Introduction

The governing equations for transient modeling of a flat plate solar collector were developed in section 3.2. These were discretized and the complete set of discretized equations along with the B.C.'s (3.14) through (3.23) were solved by finite difference technique. The computed results are presented in the following sections and are compared with the experimental data collected during the transient testing of the solar collector.

5.2 Results

The performance of flat plate solar collector for a given day, location and position depends on inputs namely mass flow rate of fluid, inlet fluid temperature, starting time, closing time and initial temperature distribution in different components of the collector.

The experiments in the present work were conducted during the winter, months namely Dec, Jan, and Feb of an year at Kanpur (India) as discussed earlier. The

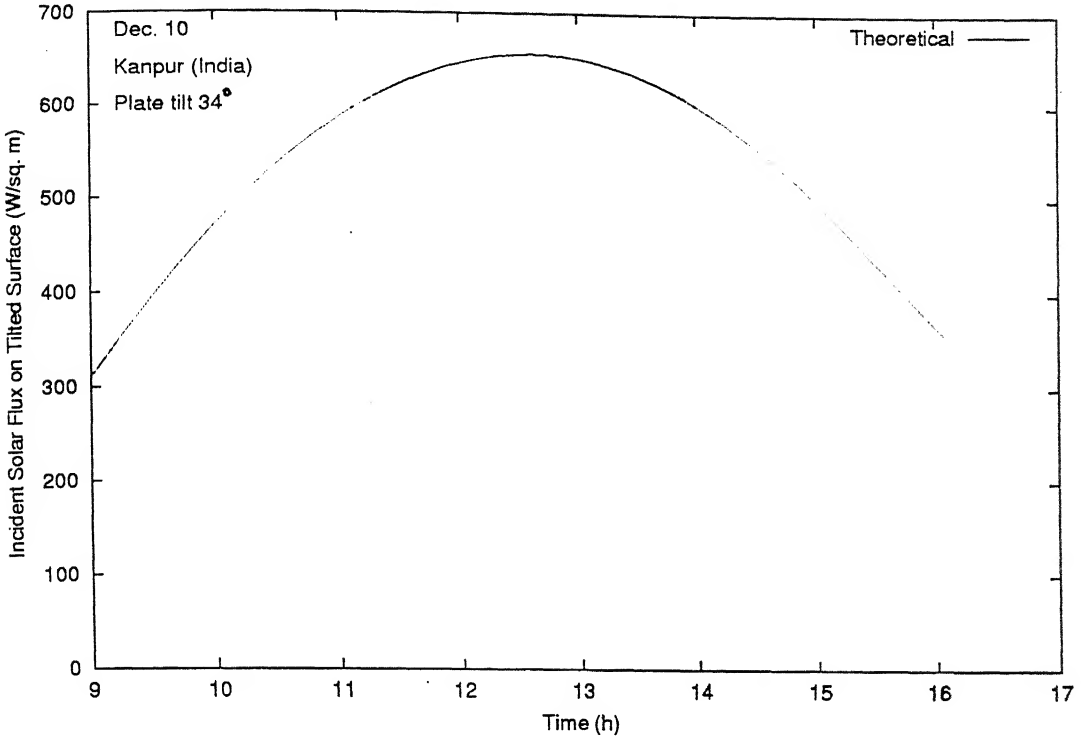

Figure 5.1: **Variation of Solar Flux on Top Cover of a Tilted Surface**

experiments were conducted from 9 A.M. to 4 P.M. The data obtained from experiments were compared with the computed results. In the experiment, the inlet temperature of the fluid and ambient temperature were continuously varying which also was considered in the theoretical model. For computations, the initial temperature distribution of different components of a flat plate collector was assumed to be same i.e. equal to the ambient temperature. The dimensions of collector, material properties and other parameter values used in computations are given in 'Appendix A'.

The variation of incident flux on the top cover of tilted flat plate collector is shown in Figure 5.1. Figures 5.2 and 5.3 show the comparison of the theoretical model results with the experimental results for single cover and double cover respectively. It gives the variation of the rise in the fluid temperature with the time of the day. For the single cover the maximum temperature rise is about 20°C and for double cover it is close to 22°C. The maximum temperature rise occurs between 12 noon and 1 P.M.

when the solar radiation flux is maximum. The above figures show good agreement between the experimental and the theoretical results from 9 A.M. to 2 P.M., but there is discrepancy during 3 P.M. to 4 P.M. This could be attributed to various factors a few of which are given below :

1. The solar insolation taken in the theoretical model may be higher than the actual values.

2. The effect of dust is not considered in the theoretical model which may affect more significantly towards the end of the day.

Figures 5.4 and 5.5 show the variation of plate mean temperature with the time of the day for single and double covers. The maximum plate temperatures are about 318 K and 319 K for single and double covers respectively. The model predicted maximum plate mean temperature was obtained between 1 P.M. and 2 P.M. Overall the model predication are in good agreement with the experimental data.

Figures 5.6 and 5.7 show the variation of instantaneous efficiency with the time of the day for single and double covers. There is a continuous decrease in efficiency with the time of the day. It is due to the increase in inlet fluid temperature while taking the experimental data as the day progresses and this aspect has been considered in the theoretical model as well. Figure 5.8 displays the nature of instantaneous efficiency with the time of the day when inlet temperature of fluid remained constant. It is seen that efficiency first rises from 9 A.M. to 11 A.M. beyond which it remains nearly constant till about 3 P.M. and then starts decreasing. This can be explained as follows. The collector is in transient state during start and much of the incident flux is absorbed by covers, absorber plate and insulation in raising their temperatures before they reach a quasi-steady state. Thus the useful energy recovered is low during this period and hence efficiency. So the period between 11 A.M. to 3 P.M. can be taken as the period during which quasi-steady state can be assumed.

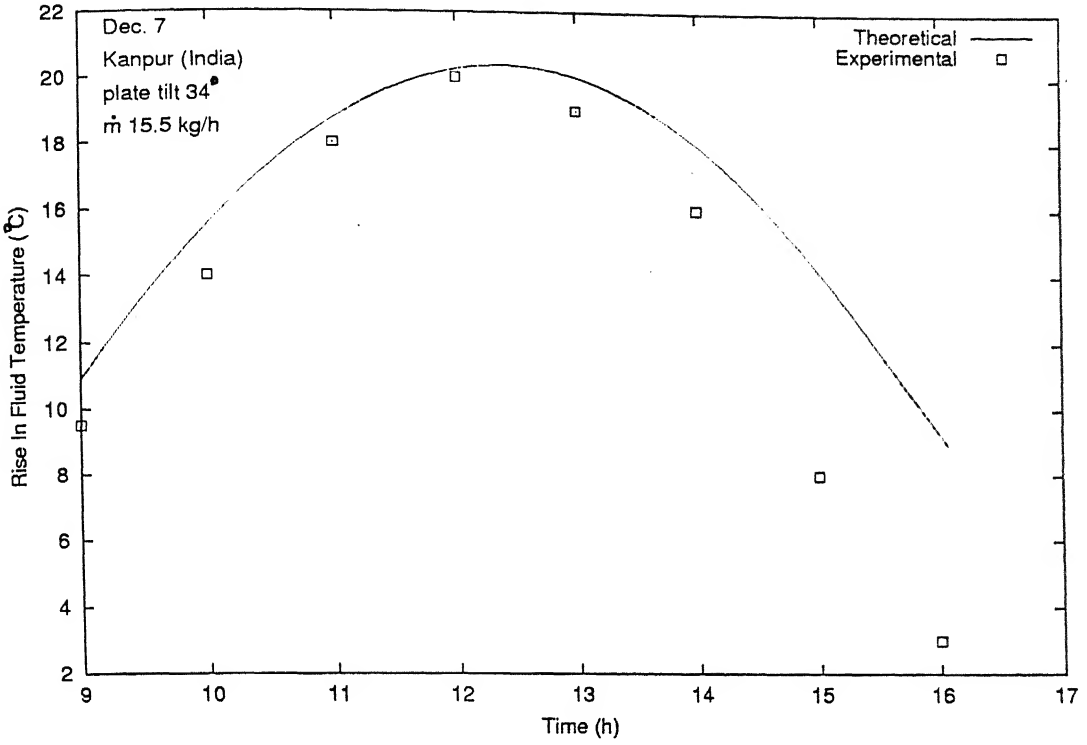

Figure 5.2: **Rise in Fluid Temperature with Single Cover**

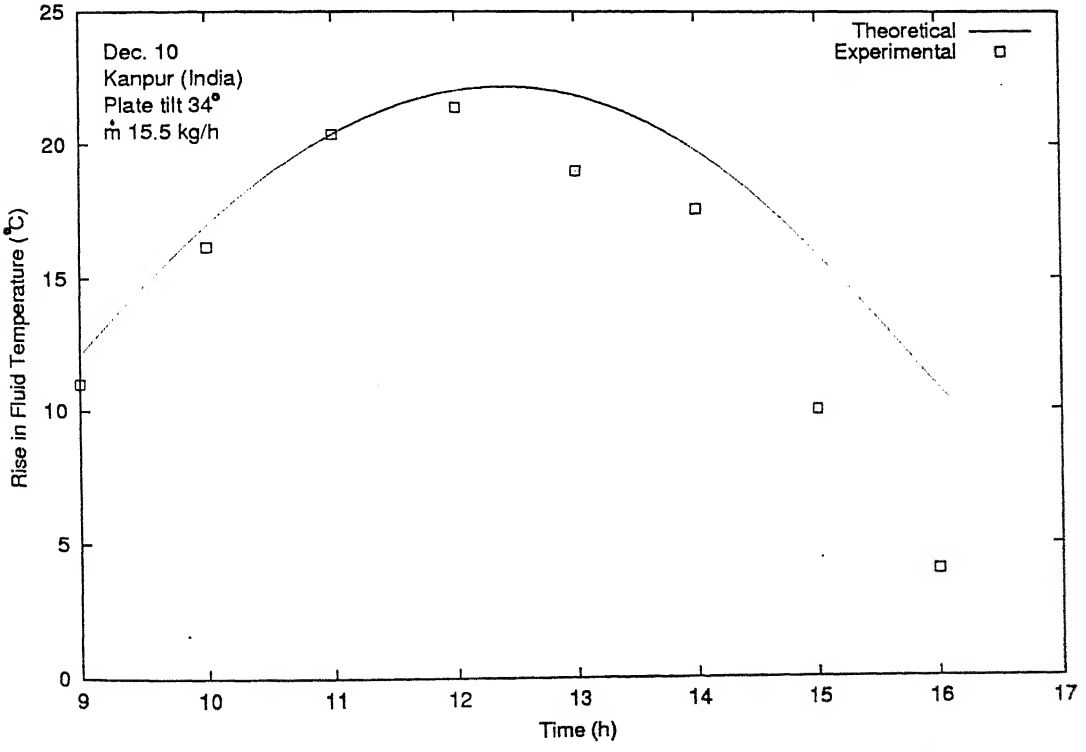

Figure 5.3: **Rise in Fluid Temperature with Double Cover**

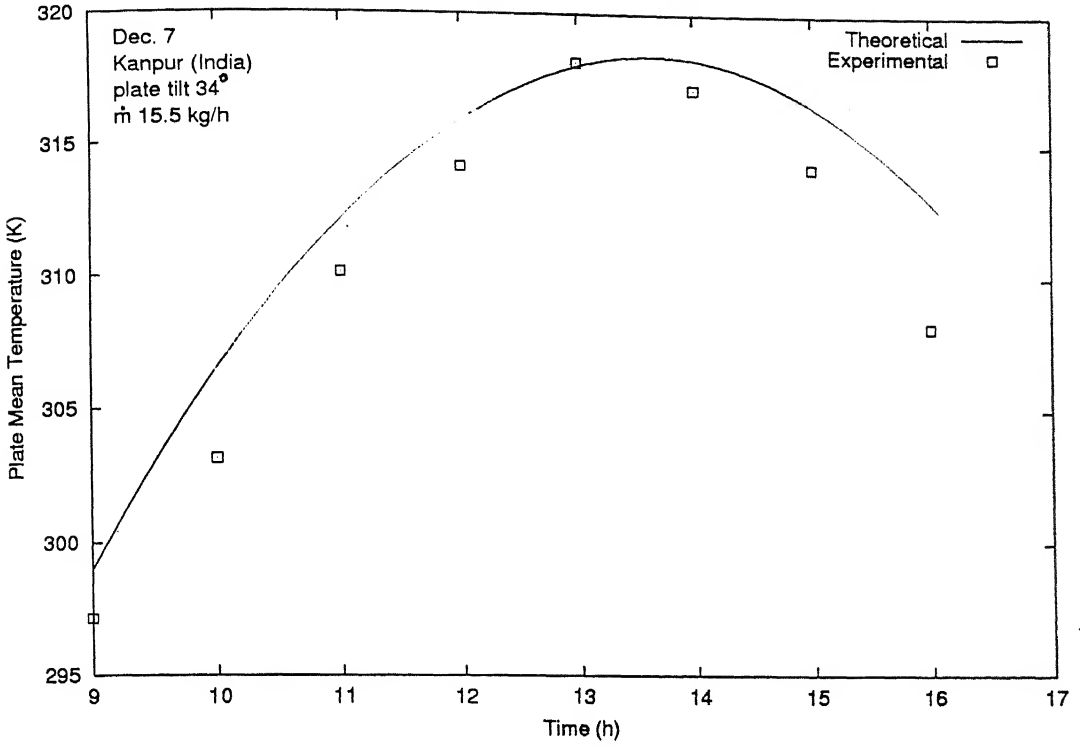

Figure 5.4: **Plate Mean Temperature with Single Cover**

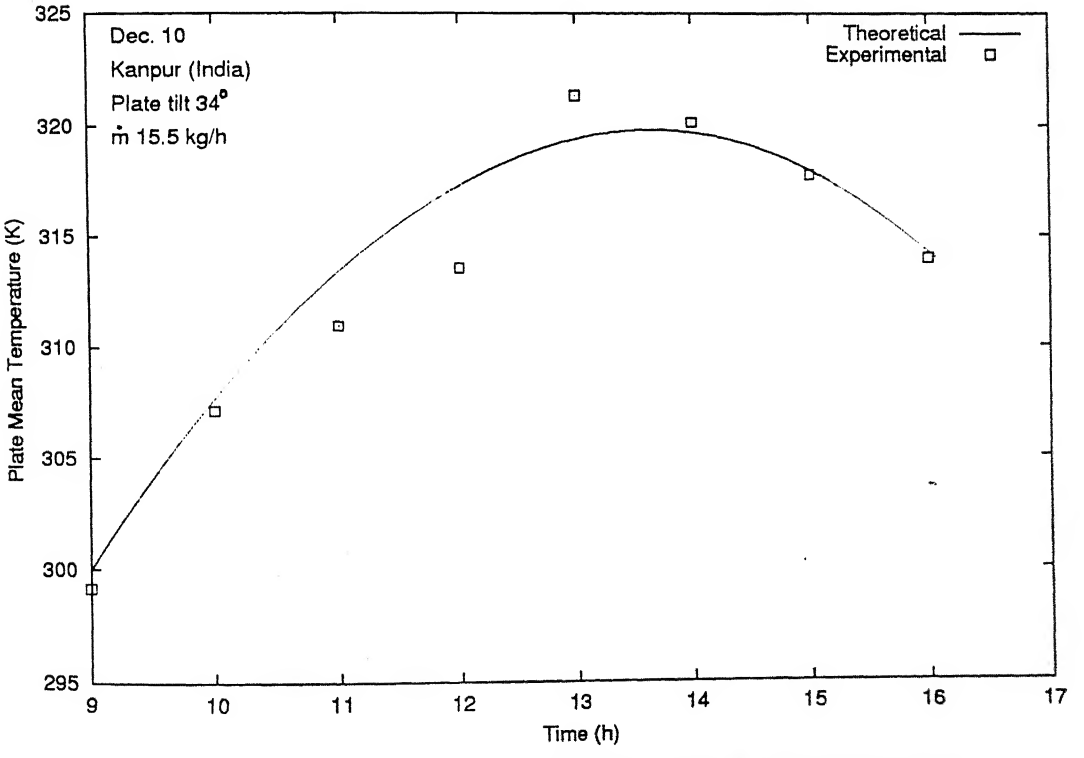

Figure 5.5: **Plate Mean Temperature with Double Cover**

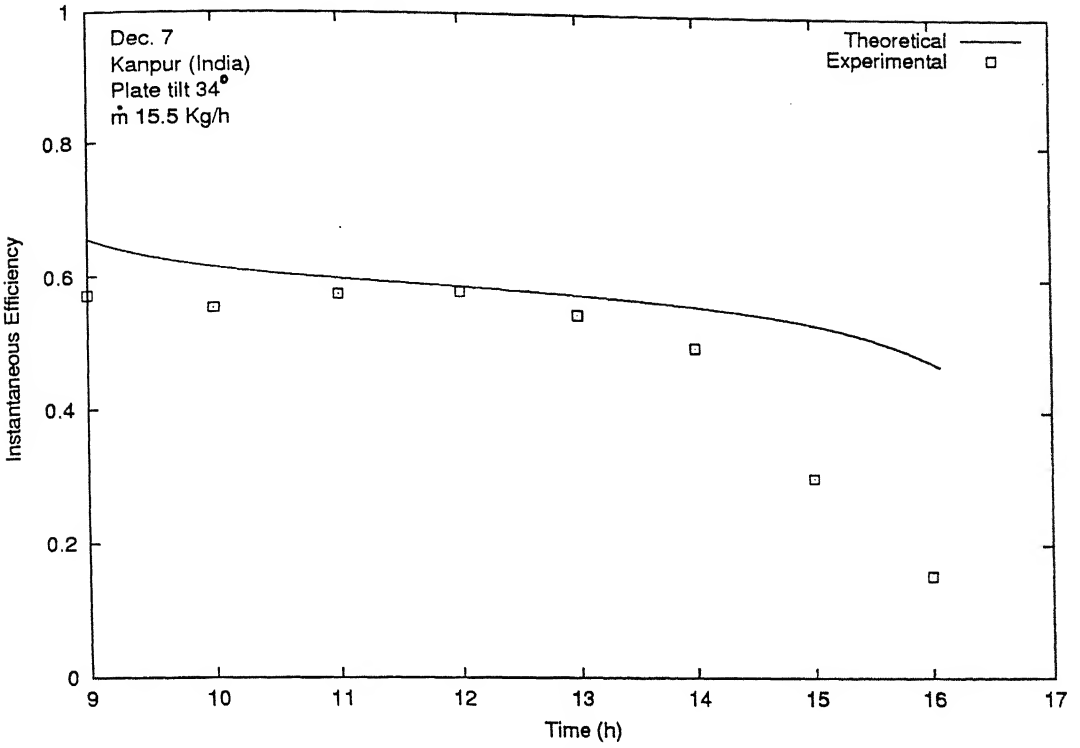

Figure 5.6: **Instantaneous Efficiency with Single Cover**

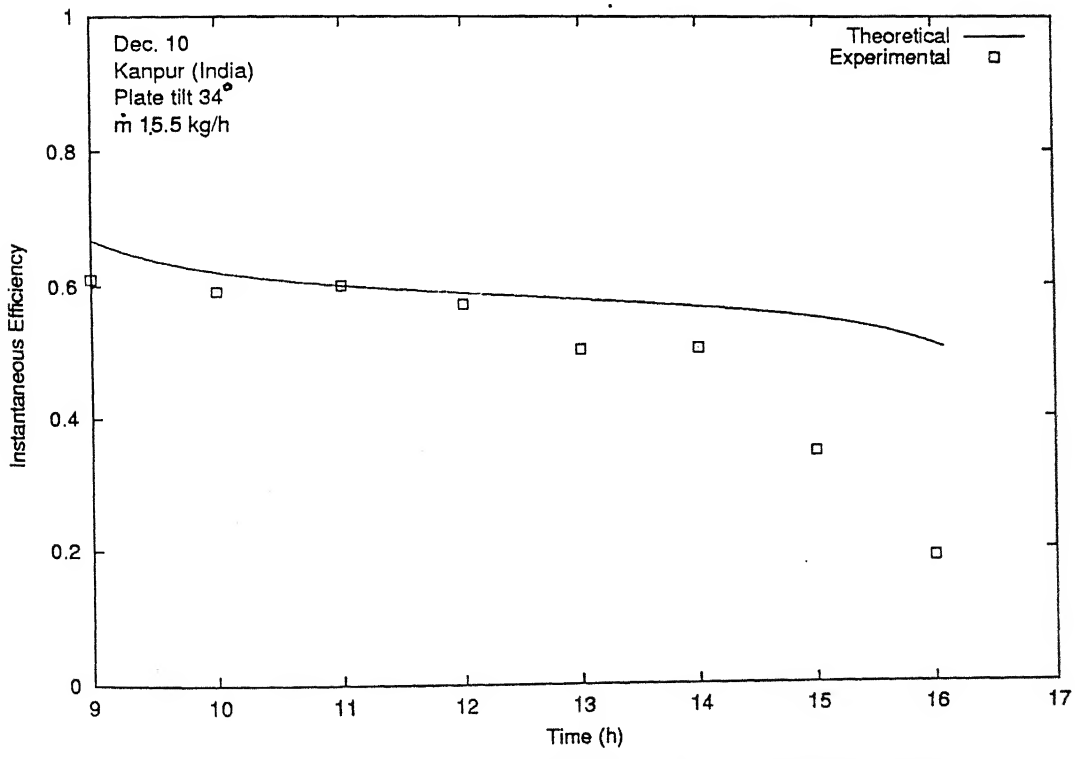

Figure 5.7: **Instantaneous Efficiency with Double Cover**

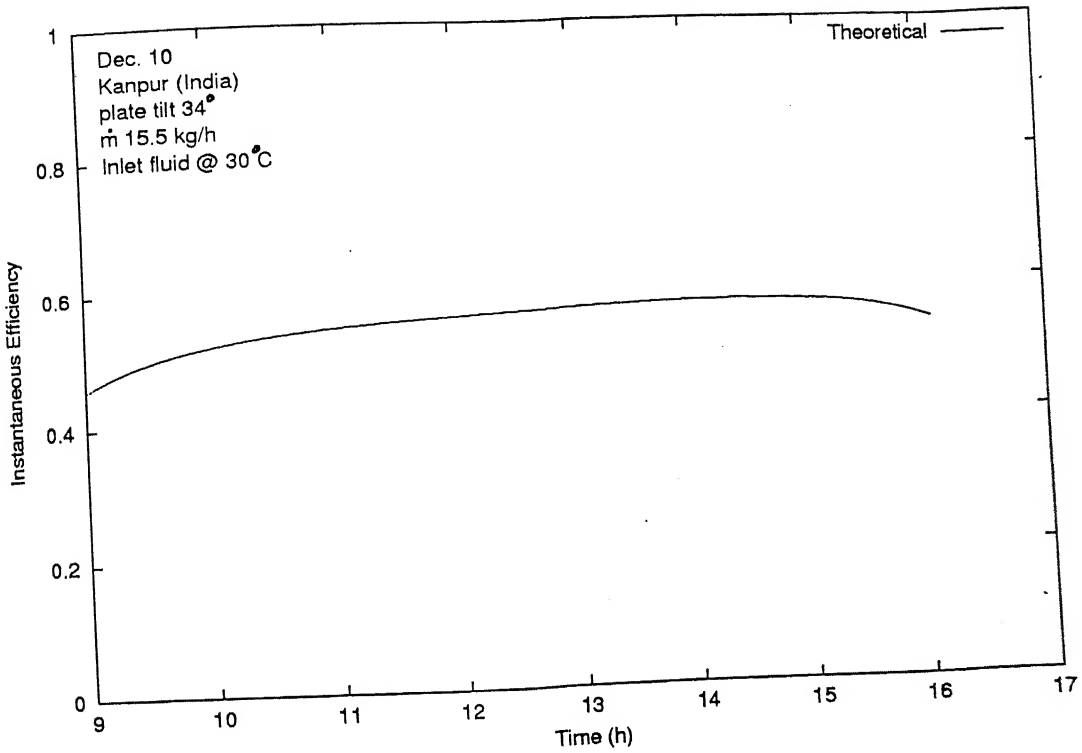

Figure 5.8: **Instantaneous Efficiency at Constant Inlet Temperature**

The inlet fluid temperature is an important parameter which strongly influences the performance of a flat plate solar collector. The effect is illustrated by plotting the mean efficiency with the inlet fluid temperature which was varied from 20°C to 60°C (see Fig. 5.9). It is observed that efficiency drops sharply at an increasing rate (from 0.65 to 0.24) with increasing inlet fluid temperature (from 20°C to 60°C) as reported in literature [31].

The flat plate collector fabricated for the experimentation used a continuous copper pipe. The temperature of fluid therefore increased continuously as it passed through. This temperature distribution of absorber plate is shown as a 3-D distribution in Fig. 5.10. Figure 5.11 shows the variation of stagnation temperature with time of the day for double cover. The experimental results show that stagnation temperature is maximum at 2 P.M. Good agreement between the experimental and theoretical values is obvious from the figure.

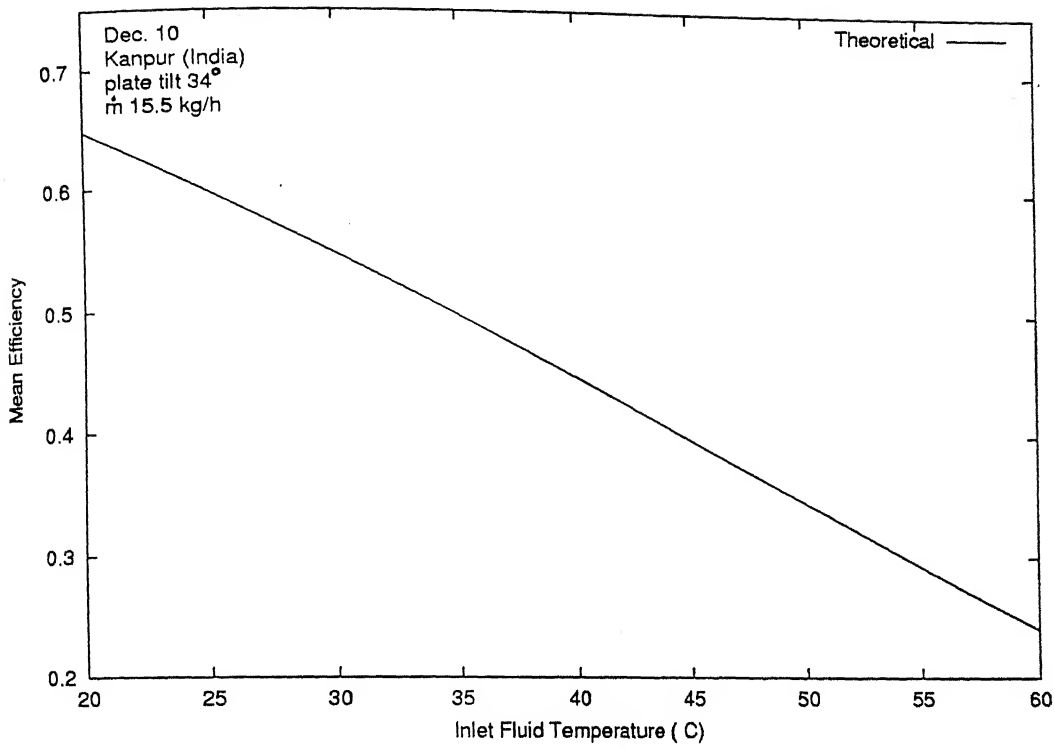

Figure 5.9: **Mean Efficiency with Inlet Fluid Temperature with Double Cover**

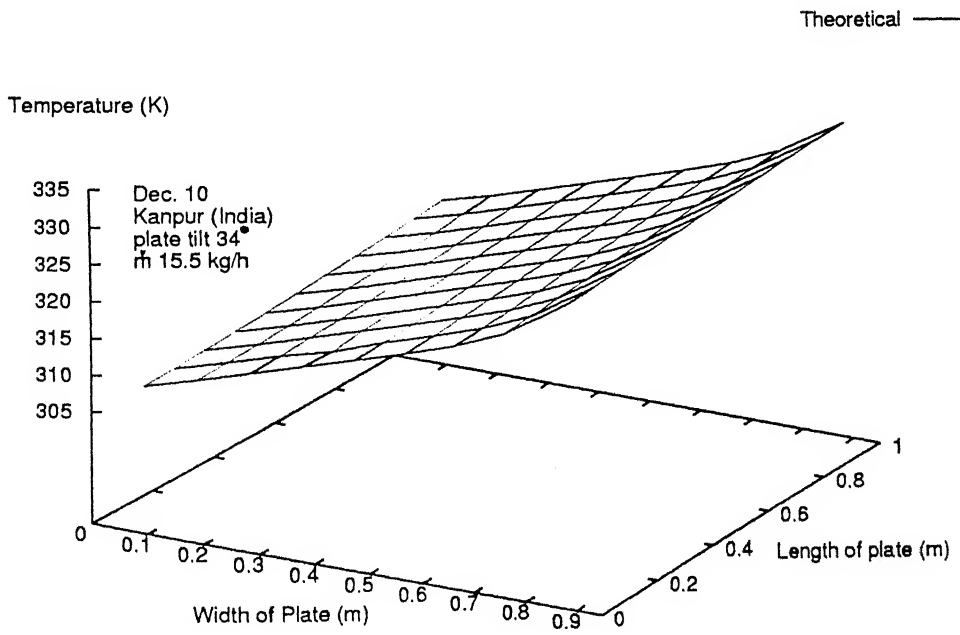

Figure 5.10: **3-D Temperature Distribution in Absorber Plate**

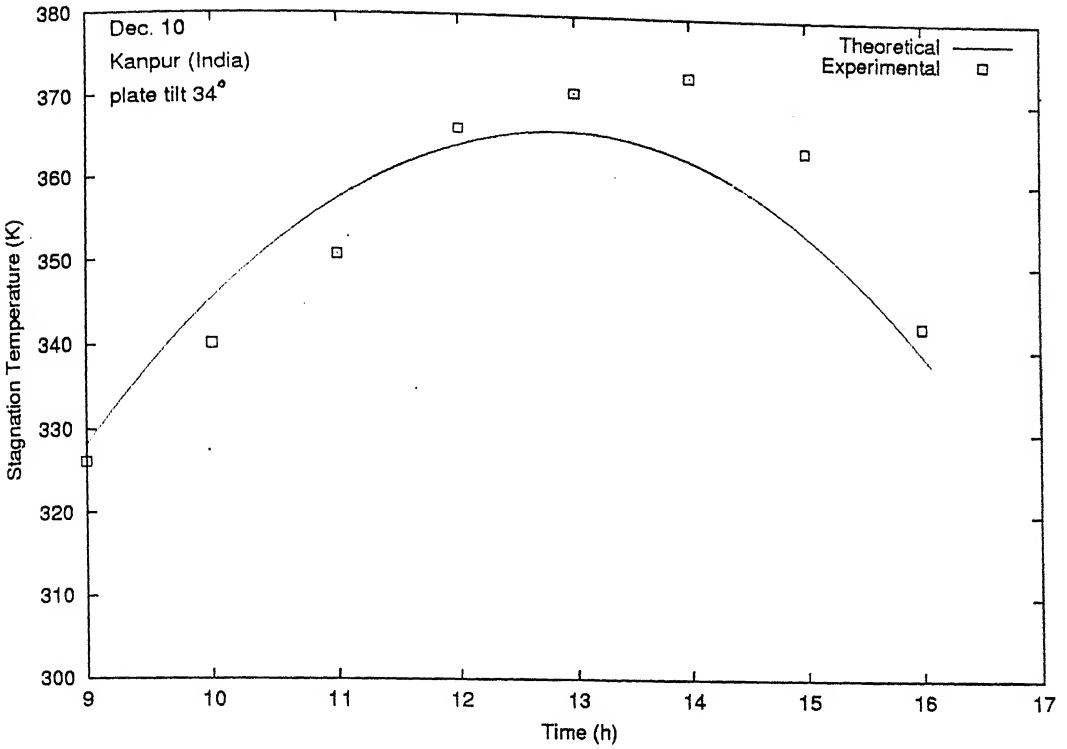

Figure 5.11: **Stagnation Temperature with Double Cover**

Figure 5.12 displays the rise in fluid temperature with time of the day for three different flow rates namely 15.5 kg/h, 31.5 kg/h and 56.5 kg/h. First the temperature rises till the noon, when the solar radiation flux is maximum. The maximum temperature rises for the lower flow rates. Figure 5.13 demonstrates the variation of plate mean temperature with the time of the day for three different flow rates. The figures 5.12 and 5.13 show good agreement between the experimental and theoretical values until 2 P.M. only after which the deviation between the two increases. Figure 5.14 shows the variation of instantaneous efficiency for the three different flow rates. The maximum efficiency is obtained for the larger flow rate. Fig. 5.15 displays the variation of mean efficiency with the mass flow rates. From the graph it is clear that mean efficiency increases as the mass flow rate increases. But for flow rates greater than 40 kg/h the mean efficiency becomes approximately constant.

Figures 5.16 and 5.17 show the variation of rise in temperature and plate mean

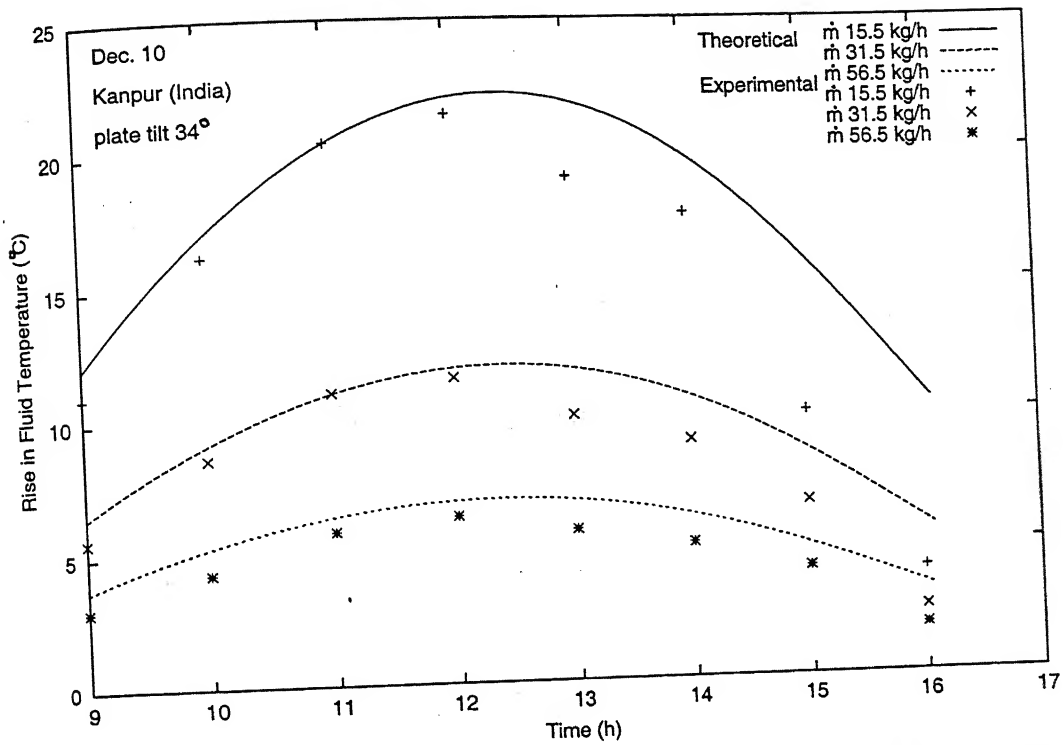

Figure 5.12: **Rise in Fluid Temperature for Different Mass Flow Rates**

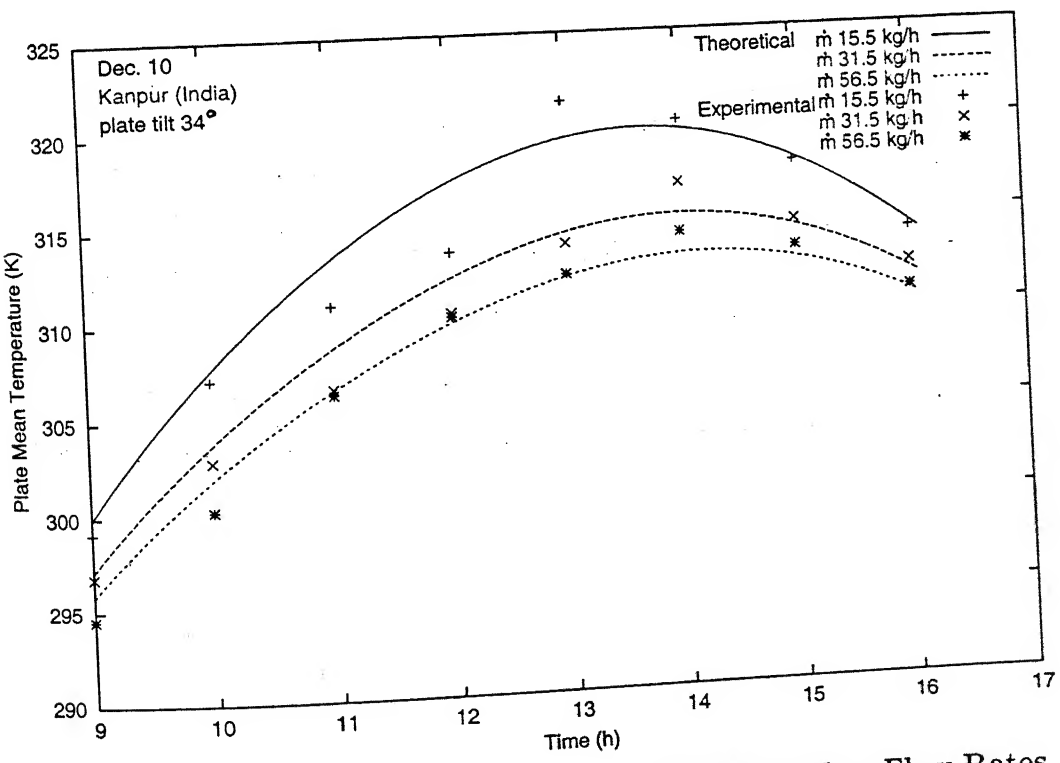

Figure 5.13: **Plate Mean Temperature for Different Mass Flow Rates**

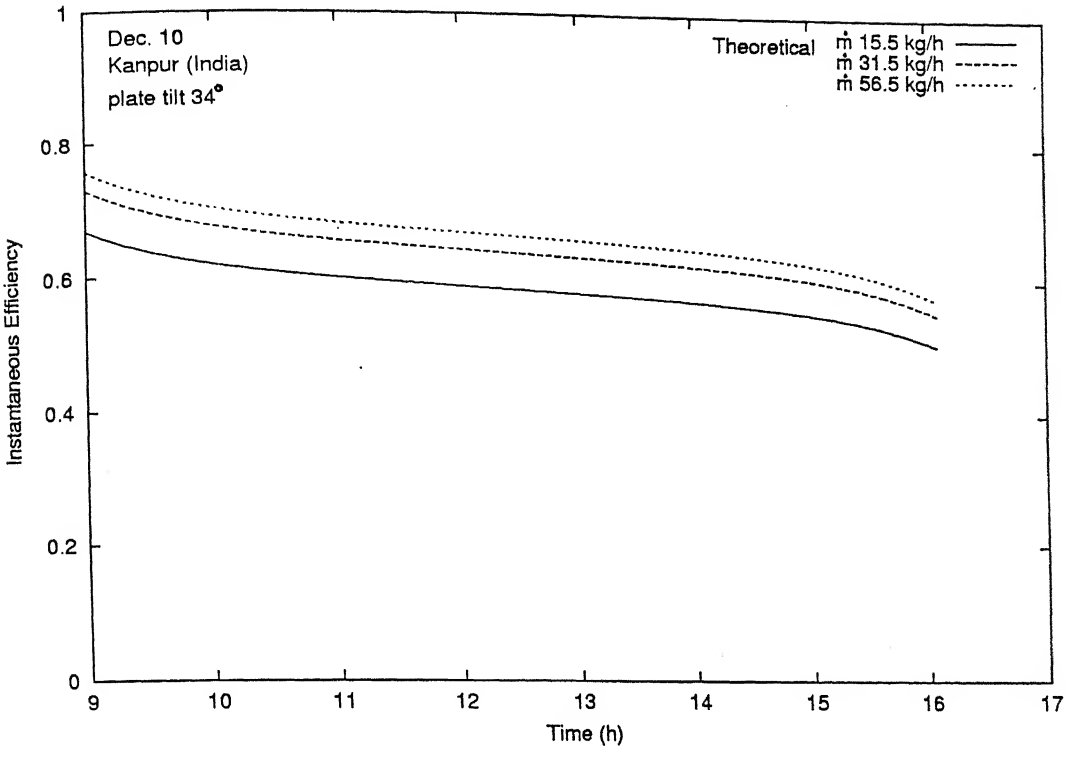

Figure 5.14: **Instantaneous Efficiency for Different Mass Flow Rates**

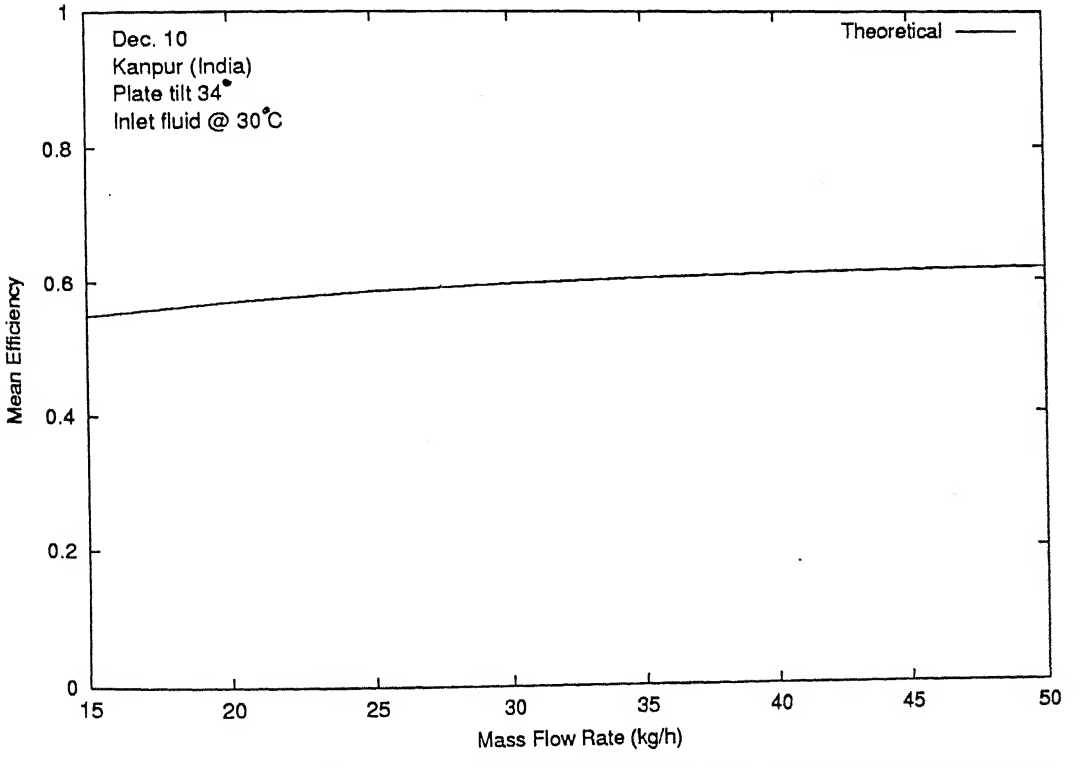

Figure 5.15: **Mean Efficiency with Mass Flow rate with Double Cover**

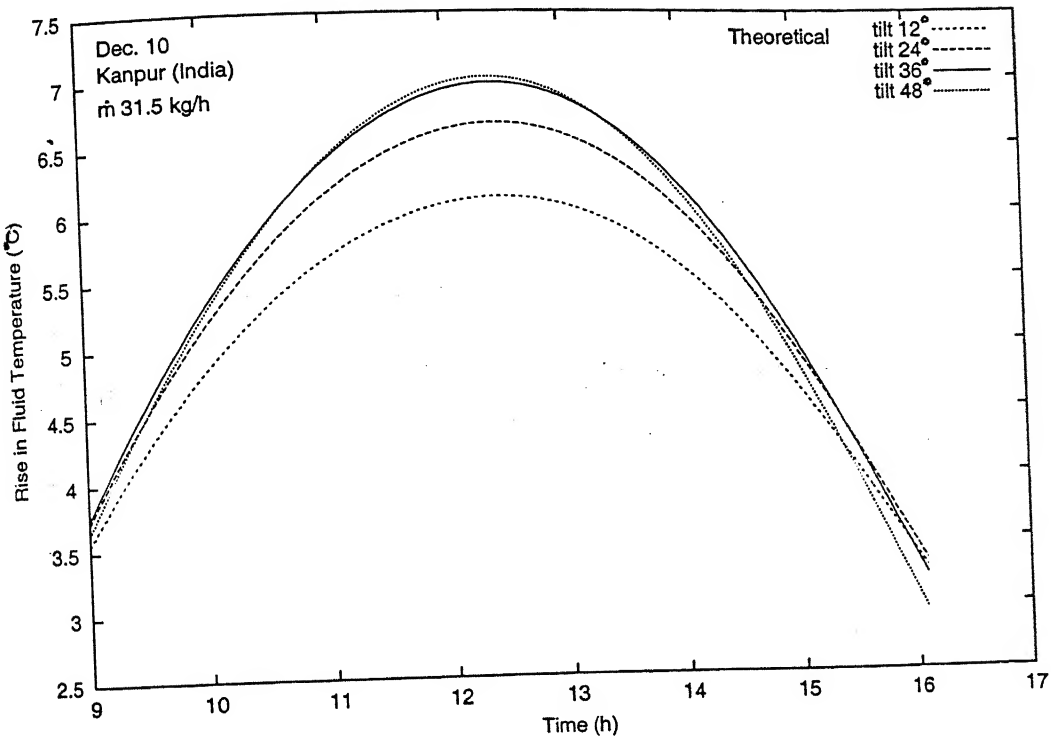

Figure 5.16: **Rise in Fluid Temperature for Different Tilt Angles**

temperature for four different tilt angles namely 12°, 24°, 36° and 48°. A tilt angle of 36° gave the maximum temperature rise and plate mean temperature for most of the time during the day. This suggests that a tilt angle of 36° i.e. $(\Phi + 10)$ may be considered as an optimum as already established in the literature [31].

Figure 5.18 shows the variation of mean efficiency with varying the distance between the plate and the cover. It is obvious from the figure that as the spacing between the cover and the plate increases the mean efficiency also increases. Fig. 5.19 shows the variation of the mean efficiency with varying the distance between the covers in a double cover design. The graph shows that greater the spacing between the covers higher in the mean efficiency. This increase in mean efficiency in Figures 5.18 and 5.19 can be attributed to the decrease in the value of convective heat transfer coefficient with increase in spacing between the plate and cover or between the two covers in a double cover design [4].

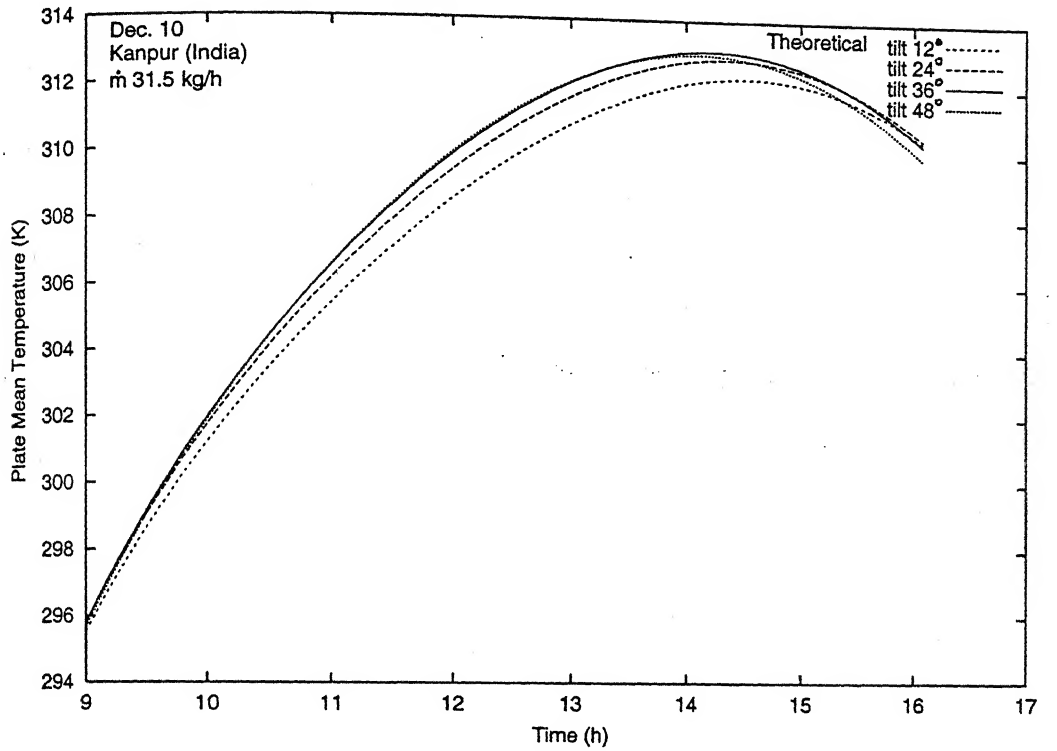

Figure 5.17: Plate Mean Temperature for Different Tilt Angles

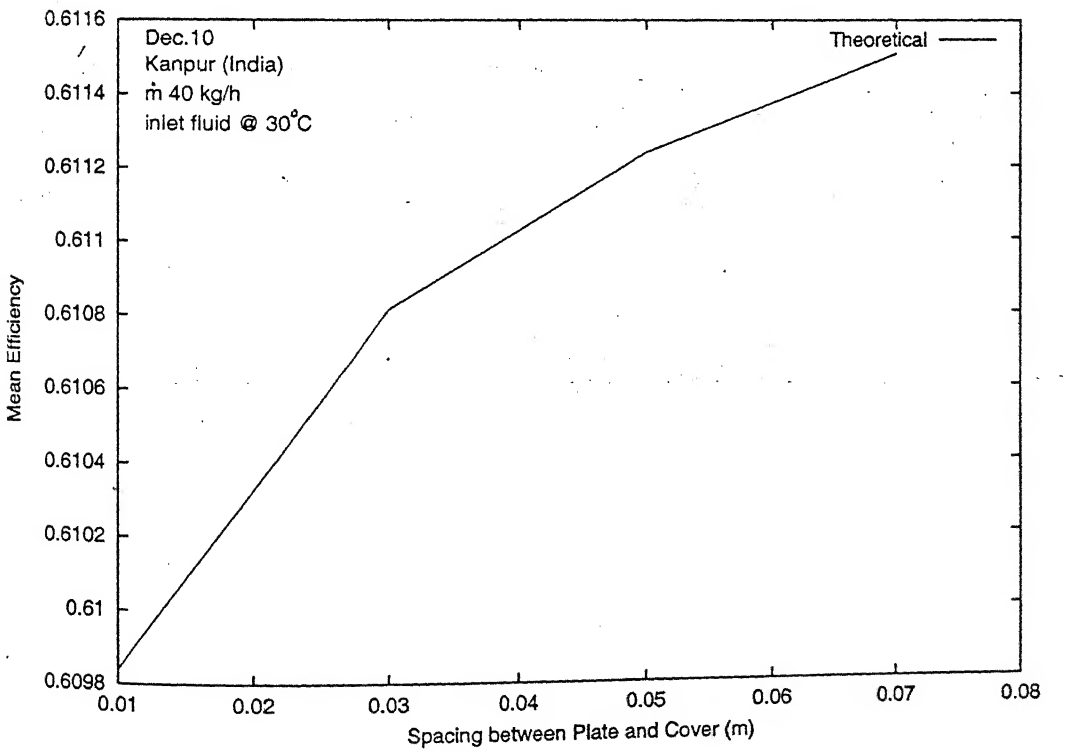

Figure 5.18: Mean Efficiency with Spacing between Plate and Cover

Figure 5.20 shows the variation of uncertainty in efficiency with the time of day. Figure shows that uncertainty is minimum at 12 noon due to maximum temperature rise that occurs at this time. The uncertainty increases after 12 noon due to progressively decreasing rise in temperature.

5.3 Conclusions

- The rise in fluid temperature is maximum between 12 noon to 1 P.M. (close to 12 noon).
- The plate mean temperature is maximum between 1 P.M. to 2 P.M. (close to 2 P.M.)
- The mean efficiency decrease as inlet temperature of fluid increases
- The mean efficiency is constant approximately for mass flow rates greater than of 40 kg/h which indicates the minimum flow rate of the collector.
- The tilt angle $\phi + 10$ is optimum tilt angle as established in literature.
- The period between 11 A.M. to 3 P.M. can be taken as the period during which quasi-steady state may be assumed for the solar collector.
- The performance of the solar collector with double cover is better than that with single cover.
- The spacing between the absorber plate and cover and between the two covers should be large. The recommended values are 50 mm to 80 mm and 50 mm respectively.
- The theoretical results are in good agreement with the experimental data from 9 A.M. to 2 P.M. which imply that the transient model developed for the flat

plate solar collector has been validated by the experimental results of the present work. This model therefore can be used to characterize a flat plate solar collector as a function of all the relevant parameters.

5.4 Suggestions for future work

- A similar transient analysis can be extended (both experimentally and theoretical) for some novel design like honeycomb collector, evacuated tube collector, plastic collectors and also with selective surfaces.
- The effect of variation of physical properties with temperature of the materials involved.
- The effect of shadow and dust on top of the collector can be investigated.
- Present model considers the temperature on the periphery of the pipe same as that of the absorber plate i.e. the thermal resistance between the plate and the pipe is neglected. The model can be extended by modeling the pipe as well similar to the other components of the collector.

APPENDIX A

The values of the parameters used are listed below :

Dimension of the collector	1.15 m×1.05 m
Width of plate	0.95 m
Length of.Plate	1 m
Thickness of the glass cover	4 mm
Thickness of absorber plate	1mm
Thickness of insulation	80 mm
Inner diameter of pipe	10.2 mm
outer diameter of pipe	12.5 mm

Material properties of the collector

Thermal conductivity of the glass covers	.078 W m^{-1} K^{-1}
Thermal conductivity of the copper absorber plate	376. W m^{-1} K^{-1}
Thermal conductivity of the glass wool insulation	.038 W m^{-1} K^{-1}
Thermal conductivity of the fluid(water)	.59 W m^{-1} K^{-1}
Specific heat of the glass covers	840 J kg^{-1} K^{-1}
Specific heat of the absorber plate	383.1 J kg^{-1} K^{-1}
Specific heat of the insulation	700 J kg^{-1} K^{-1}
Specific heat of the fluid	4187 J kg^{-1} K^{-1}
Density of the glass cover	2700 kg m^{-3}

Density of the absorber plate	8954 kg m^{-3}
Density of the insulation	24 kg m^{-3}
Density of the fluid	1000 kg m^{-3}
Refractive index of glass relative to air	1.526
Extinction coefficient of glass	6.8504 m^{-1}
Reflectivity of the surrounding	0.2
Latitude of kanpur	26.28°

Discretization grids

Cover2	11×11
Cover1	11×11
Absorber plate	11×11
Insulation	11×11×11
Fluid	11
Δt	10 s

Bibliography

[1] Amer E.H., Nayak J.K. and Sharma G.K., 1997, "Transient test methods for flat-plate collectors : Review and experimental evaluation", Solar Energy, Vol.60, pp. 229-243.

[2] Behnia M. and Morrison G.L., 1991 "An experimental investigation of inclined open thermosyphons", Solar Energy, Vol.47, pp. 313-326

[3] Bhide V.G., Vaishya J.S., Nagar V.K. and Sharma S.K., 1982, "Choice of selective coating for flat plate collectors", Solar Energy, Vol.29 , pp. 463-465.

[4] Buchberg H., Catton I. and Edwards D.K., 1976, "Natural convection in enclosed spaces - A review of applications to solar energy collection", Journal of Heat Transfer,Trans. ASME, Vol.98, pp. 182.

[5] Chiou J.P., 1982, "The effect of nonuniform fluid flow distribution on the thermal performance of a solar collector", Solar Energy, Vol.29, pp. 487-502.

[6] Choudhury B., 1982, "A parameterized model for global insolation under partially cloudy skies", Solar Energy, Vol.29, pp. 479-486.

[7] Coleman H.W. and Steele W.G., 1989, "Experimentation and uncertainty analysis for engineers", John wiley & Sons, Newyork, USA.

[8] De Ron A.J., 1980, "Dynamic modeling and verification of a flat-plate solar collector", Solar Energy, Vol.24, pp. 117-128.

[9] Duffie J.A. and Beckman W.A., 1974 "Solar energy thermal processes", John Wiley, New York.

[10] Gani R. and Symons J.G., 1979, "Cover systems for high temperature flat-plate solar collectors", Solar Energy, Vol.22, pp. 555-561.

[11] Gutierrez G., Hincapie F., Duffie J.A. and Beckman W.A., 1974, "Simulation of forced circulation water heaters; effects of auxiliary energy supply, load type and storage capacity", Solar Energy, Vol.15, pp. 287-298.

[12] Garg H.P., 1974, "Effect of dirt on transparent covers in flat-plate solar energy collectors", Solar Energy, Vol.15, pp. 299-302.

[13] Hobson P.A. and Norton B., 1988, "Verified accurate performance simulation model of direct thermosyphon solar energy water heaters", Journal of Solar Energy Engineering, Trans. ASME, Vol.110, pp. 282.

[14] Hottel, H.C. and Woertz, B.B., 1942, "The performance of flat-plate solar-heat collectors", Trans. ASME Vol.64, pp. 91-99.

[15] Iqbal M., 1966, "Free-convection effects inside tubes of flat-plate solar collector", Solar Energy, Vol.10, pp. 207-211.

[16] Jenkins J.P. and Hill J.E., 1980, "A comparison of test results for flat-plate water-heating solar collectors using BSE and ASHARE procedures", Journal of Solar Energy Engineering, Trans. ASME, Vol.102, pp. 2.

[17] Klein S.A., Duffie J.A. and Beckman W.A., 1974, "Transient consideration of flat-plate solar collectors", Trans. ASME, J. of Engineering for Power, Vol.96, pp. 109-113.

[18] Klein S.A., Cooper P.I., Freeman T.L., Beckman W.A. and Duffie J.A., 1975, "A method of simulation of solar processes and its application", Solar Energy, Vol.17, pp. 29-37.

[19] Mani A., 1980, "Handbook of Solar Radiation Data for India, Allied Publishers", New Delhi.

[20] Morrison G.L., Gilliaert D. and Tebaldi P., 1992, "Outdoor testing of solar water Heaters -Effect of load pattern and auxiliary boosting", Solar Energy, Vol. 49, pp. 299-308.

[21] Morrison G.L. and Ranatunga D.B.J., 1980, "Transient Response of Thermosyphon Solar Collectors", Solar Energy, Vol.24, pp. 55-61.

[22] Nayak J.K., Sukhatme S.P., Limaye R.G. and Bopshetty S.V., 1989, "Performance studies on solar concrete collectors", Solar Energy, Vol.42, pp. 45-56.

[23] Nordgaard A. and Beckman W.A., 1992, "Modelling of flat-plate collectors based on monolithic silica aerogel", Vol.49, pp. 387-402.

[24] Oliva A. and Costa M., 1991, "Numerical simulation of solar collector : The effect of nonuniform and nonsteady state of boundary conditions", Solar Energy, Vol.47, pp. 359-374.

[25] Onyegegbu S.O. and Morhenne J., 1993, "Transient multidimensional second law analysis of solar collectors subjected to time-varying insolation with diffuse components", Solar Energy, Vol.50, pp. 85-95.

[26] Pierson P., Padet J., 1990, "Time constant of solar collectors", Solar Energy, Vol.44, pp. 109-114.

[27] Russel L.D. and Guven H.M., "Modeling and analysis of an All-plastic flat-plate collector", Journal of Solar Energy Engineering,Trans. ASME, Vol.104, pp. 333.

[28] Saito A., Utaka Y., Tsuchio T. and Katayama K., 1984, "Transient response of flat-plate solar collectors for periodic solar intensity variation ", Solar Energy, Vol.32, pp. 17-23.

[29] Sparrow E.M. and Tien K.K., 1977, "Free convection heat transfer at an inclined and yawed square plate-application to solar collectors", Journal of Heat Transfer,Trans. ASME, Vol.99, pp. 507.

[30] Srivastava N.K. and Kant K., 1998, "Multidimensional Transient Simulation of a Flat Plate Solar Collector", Proceeding of international conference on Energy Research and Development held at state of Kuwait, Nov. 9-11, 1998, Vol.II, pp. 979-990.

[31] Sukhatme S.P., 1996, "Solar Energy", Tata McGraw-Hill, New Delhi, 2 edition.

[32] Tannehill J.C., Anderson D.A., Pletcher R.H., 1997, "Computational Fluid Mechanics and Heat Transfer", Taylor & Francis Publication USA, 2 edition.

[33] Thomas W.C., Dawson A.G., Waksman D. and Streed E.R., 1982, "Incident angle modifiers for flat plate solar collectors: Analysis of measurement and calculation procedures",Journal of Solar Energy Engineering,Trans. ASME, Vol.104, pp. 349.

[34] Threlkeld J.L., 1962, "Thermal Environmental Engineering", Prentice-Hall, INC , USA.

[35] Veziroglu T.N., 1981, "Alternative energy sources II", Vol.1, Solar Energy 1. McGraw-Hill, USA.

[36] Zhao Q., Sadler G. W. and Leonard J.J., 1988, "Transient simulation of flat-plate solar collectors", Solar Energy, Vol.40, pp. 167-174.